

Alma Mater Studiorum – Università di Bologna

DOTTORATO DI RICERCA
BIOTECNOLOGIE CELLULARI E MOLECOLARI
Ciclo XXII

Settore/i scientifico disciplinari di afferenza: BIO/10

MODULATION OF EPIDERMIAL GROWTH FACTOR RECEPTOR
SIGNALING IN COLON ADENOCARCINOMA.

Presentata da: Johana Hysomema

Coordinatore Dottorato

Chiar.mo Prof. Lanfranco Masotti

Relatore

Chiar.mo Prof. Lanfranco Masotti

Esame finale anno 2010

TABLE OF CONTENTS

ABSTRACT	4
1. INTRODUCTION	5
1.1 INTRODUCTION TO CANCER	6
1.2 COLORECTAL CANCER (CRC)	7
1.2.1 <i>Histopathology of colorectal cancer development</i>	7
1.2.2 <i>Biology of colorectal cancer</i>	9
1.2.3 <i>Colorectal cancer staging</i>	13
1.2.3 <i>CRC treatment</i>	14
1.3 EPIDERMIAL GROWTH FACTOR RECEPTOR	17
1.3.1 <i>Biochemical and structural characterisation of EGFR ...</i>	18
1.3.2 <i>EGFR: Signaling and trafficking</i>	20
1.4 EGFR ROLE IN CANCER	24
1.5 AIM OF THE RESEARCH.....	27
2. TECHNIQUES.....	28
2.1 CONFOCAL LASER SCANNING MICROSCOPY.....	29
2.2 SURFACE PLASMON RESONANCE BIOSENSORS (BIACORE).....	33

3. MATERIALS AND METHODS	38
3.1 CELL CULTURE AND TREATMENTS	39
3.2 CELL PROLIFERATION ASSAY	40
3.3 CONFOCAL LASER SCANNING MICROSCOPY	40
3.4 FLOW CYTOMETRY ANALYSIS	41
3.5 EGFR PHOSPHORILATION STATE ANALYSIS.....	42
<i>3.5.1 Treatments</i>	<i>42</i>
<i>3.5.2 Protein extraction: whole cell lysate</i>	<i>42</i>
<i>3.5.3 Determination of protein concentration.....</i>	<i>42</i>
<i>3.5.4 Immunoprecipitation and Western Blot.....</i>	<i>43</i>
3.6 EGF/EGFR COMPLEX INTERACTION STUDIES	
BY SURFACE PLASMON RESONANCE.....	44
<i>3.6.1 EGFR capturing from A431 total cell lysate and</i>	
<i>binding to EGF</i>	<i>44</i>
<i>3.6.2 EGF immobilization and binding to EGFR</i>	<i>46</i>
<i>3.6.3 Purified EGFR immobilization and binding to EGF....</i>	<i>46</i>
4. RESULTS	48
4.1 CELL VIABILITY ASSESMENT.....	49
4.2 FR18 EFFECTS ON EGF/EGFR INTERACTION.....	50
4.3 CELL CYCLE ANALYSIS AND APOPTOSIS	
EVALUATION	51

4.4 EFFECTS OF FR18 ON EGFR PHOSPHORYLATION..	53
4.5 SPR STUDIES OF EGF/EGFR INTERACTION	54
<i>4.5.1 EGF binding to captured and reconstituted EGFR</i>	
<i>from A431 cell lysate</i>	54
<i>4.5.2 Immobilised EGF interaction with A431 cell lysate</i>	57
<i>4.5.3 EGF binding to amine coupled purified EGFR</i>	59
5. DISCUSSION.....	61
6. BIBLIOGRAPHY	64
ATTACHMENT I: PhD COURSE 2007-2009, LIST OF CONGRESS PARTICIPATIONS	75

ABSTRACT

The use of agents targeting EGFR represents a new frontier in colon cancer therapy. Among these, monoclonal antibodies (mAbs) and EGFR tyrosine kinase inhibitors (TKIs) seemed to be the most promising. However they have demonstrated low utility in therapy, the former being effective at toxic doses, the latter resulting inefficient in colon cancer. This thesis work presents studies on a new EGFR inhibitor, FR18, a molecule containing the same naphthoquinone core as shikonin, an agent with great anti-tumor potential. In HT-29, a human colon carcinoma cell line, flow cytometry, immunoprecipitation, and Western blot analysis, confocal spectral microscopy have demonstrated that FR18 is active at concentrations as low as 10 nM, inhibits EGF binding to EGFR while leaving unperturbed the receptor kinase activity. At concentration ranging from 30 nM to 5 μ M, it activates apoptosis. FR18 seems therefore to have possible therapeutic applications in colon cancer.

In addition, surface plasmon resonance (SPR) investigation of the direct EGF/EGFR complex interaction using different experimental approaches is presented. A commercially available purified EGFR was immobilised by amine coupling chemistry on SPR sensor chip and its interaction to EGF resulted to have a $K_D = 368 \pm 0.65$ nM. SPR technology allows the study of biomolecular interactions in real-time and label-free with a high degree of sensitivity and specificity and thus represents an important tool for drug discovery studies. On the other hand EGF/EGFR complex interaction represents a challenging but important system that can lead to significant general knowledge about receptor-ligand interactions, and the design of new drugs intended to interfere with EGFR binding activity.

1. INTRODUCTION

1.1 INTRODUCTION TO CANCER

Cancer is a heterogeneous group of diseases in which a single cell, following mutations of genes that control cell growth, genetic stability and sensitivity to programmed cell death, acquires the ability to proliferate abnormally resulting in an accumulation of progeny. Usually, the mutation arises as a result of environmental factors such as chemicals, radiation or viruses and less than 10% of all cancer mutations are inherited.

Cancer is, in essence, a genetic disease that originates through a multistep process. In this model, the first stage, the initiation, is caused by the acquisition in a cell of a mutation that can provide a growth advantage and/or irreversible alterations in cellular homeostasis and differentiation. Three important steps involved in initiation are carcinogens (very often chemical agents), DNA repair, and cell proliferation. Many chemical agents must be metabolically activated before they become carcinogenic and most of them are strong electrophiles and bind to DNA to form adducts that must be removed by DNA repair mechanisms. Hence, DNA repair is essential to reverse adduct formation and to prevent DNA damage. Failure to repair chemical adducts, followed by cell proliferation, results in permanent alterations or mutation(s) in the genome that can lead to oncogene activation or inactivation of tumor suppressor genes. Proto-oncogenes encode proteins that promote cell growth, thus their alteration can result in the expression of a protein with impaired function or in abnormal expression (typically an over expression) of the normal protein that determines a continuous stimulation of cell proliferation. The products of tumor suppressor genes, instead, inhibit the uncontrolled proliferation and the damage of both normal alleles is necessary for the neoplastic transformation.

The next step, the promotion, can be a potentially reversible or interruptible clonal expansion of the initiated cell by a combination of growth stimulation and inhibition of apoptosis. Further progression steps occur upon clonal expansion of the initial cells and accumulation of a sufficient number of mutations and epigenetic alterations to acquire growth stimulus-independency and resistance to growth inhibitors and apoptosis, ultimately leading to an unlimited replicative potential. The acquisition of the ability to invade the surrounding tissue defines the malignant character of cancer cells, while the process through which cells can migrate to distal organs and acquire the potential to form metastasis represents the achievement of a full malignant cancerous phenotype.

1.2 COLORECTAL CANCER (CRC)

Colorectal cancer is the third most common cancer in both men and women [1]. It remains one of the most frequent and deadly diseases despite important advantages in treatment and diagnosis. The most prominent risk factors for CRC are represented by obesity, physical inactivity, alcoholism, smoking, and a diet that is high in fats or low in fruits and vegetables [2]. Environmental factors presumably modulate the risk for genetic mutations responsible for CRC, although the precise molecular mechanisms currently are unknown. The evolution from normal colonic mucosa to adenoma with different grades of dysplasia and finally to invasive cancer (adenoma-to-carcinoma sequence) is associated with a series of genetic events occurring over an 8- to 11-year time frame [3]. Not surprisingly, the incidence of colorectal cancer increases with age, especially after 60 years [4]. There appears to be an acceleration of this process in familial adenomatous polyposis (FAP) and hereditary nonpolyposis CRC (HNPCC), the two major forms of hereditary CRC.

FAP makes up 1%-2% of hereditary CRC [5], and arises from genetic mutations in the adenomatous polyposis coli (APC) gene, whose protein end product plays a key role in the Wnt/ β -catenin signaling pathway. HNPCC accounts for approximately 5%-8% of the hereditary forms of CRC, and it is caused by genetic mutations in the family of mismatch repair (MMR) genes, which include *MLH1*, *MSH2*, *MSH6*, and *PMS2* that preserve genomic integrity. In fact, germline mutations in one of these four MMR genes have been identified in up to 80% of affected families [6].

In contrast to hereditary CRC, which makes up approximately 8%-15% of all cases of CRC, sporadic CRC accounts for nearly 85%-90% of cases. The significant insights gained from studying inherited CRC, however, have contributed greatly to the current understanding of sporadic disease.

1.2.1 Histopathology of colorectal cancer development

The digestive surface of the human large intestine is characterized by a monolayer of specialized epithelial cells that forms invaginations called crypts. At the base of each crypt 4-6 intestinal stem cells are located from which the four cellular types that constitute the intestinal layer originate: columnar absorptive cells, the mucussecreting goblet cells, the neuroepithelial cells and the Paneth cells. By asymmetrical division, these stem cells are able to renew the complete layer in 3-8 days.

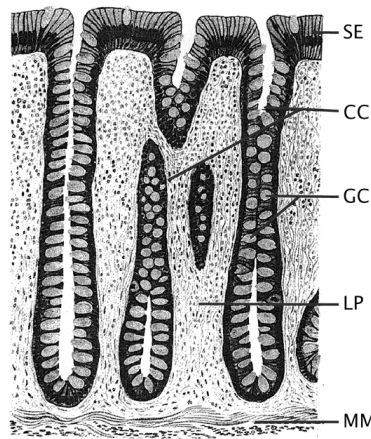


Figure 1.2.1: Morphology of normal colon tissue (cross section). Surface epithelium (SE), colon crypts (CC), goblet cells (GC), lamina propria (LP), and muscularis mucosa (MM). Figure has been reproduced from [7].

The first recognisable manifestation of epithelial alteration during colorectal tumor development are the aberrant crypt foci (ACF), small hyper- or dysplastic lesions characterized by: 1) bigger size than the normal crypts; 2) increased pericryptal space that separates them from the normal crypts; 3) a thicker layer of epithelial cells that often stains darker compared with normal crypts; 4) generally oval rather than circular openings. The ACF can be observed as single altered crypts or as a group of altered crypts that appears to form a single unit or focus. They frequently are microscopically elevated above the mucosa but also may be depressed, i.e., they usually are not in the same focal plane as the surrounding normal crypts [8, 9].

From a practical perspective, although only a small number of ACF will ultimately progress to CRC, larger ACF with altered morphology, dysplastic histology and associated gene mutations remain high-risk candidates for adenoma and CRC formation [10].

Upon increase of birth/loss ratio among epithelial cell, their progressive accumulation results in a benign tumor mass or polyp (abnormal accumulation of cells). In the intestine, a tumor is clinically recognized as a protrusion into the lumen from the wall. From a histological perspective, there are at least two major types of polyps: the hyperplastic or non-neoplastic polyp and the dysplastic or adenomatous polyp. Whether the first kind of lesion consists of large number of cells with a normal morphology that line up in a single row, the adenomatous polyp is represented by abnormal cells which show intracellular and intercellular irregularities, with disruption of normal tissue architecture. The nuclei of these cells are often hyperchromatic and larger in size than in normal intestinal cells, with irregular positioning along the crypt-villus axis due to loss of cell polarity and nuclear stratification. Several layers of these abnormal cells give rise to branching glands on the *lamina propria* (the connective tissue layer that supports the epithelium). According to their architecture, adenomas may be divided in tubular, when coarsely lobulated and pedunculated, or

villous, when sessile, covering a broad area directly onto the *muscularis mucosae* (the muscle layer underlying the epithelial lining) and submucosa (the underlying stromal layer). Villous adenomas are thought to have higher risk of malignant progression [11].

When an adenoma progresses, more undifferentiated cells appear, with a marked pleomorphism (variation in size and shape) and a nuclear:cytoplasm ratio close to 1. Moreover, tumor cells show aberrant orientations and grow in disorganized fashion. These lesions can also be referred to as carcinoma *in situ*, i.e. advanced high dysplastic lesions still confined within the epithelial layer. Finally, malignant adeno-carcinomas are characterized by the ability to invade the surrounding tissues through the *muscularis mucosae* and into the stromal compartment, and migrate to distal organs (e.g. the liver) where they can form metastasis [12].

The development of carcinoma from adenomatous lesions, also referred as adenoma-to-carcinoma sequence, is substantiated by a number of epidemiologic, clinical, pathologic, and molecular genetic observations. First, the peak of incidence of adenomatous polyps precedes by some years that of colorectal cancer; secondly, small carcinomatous foci are found within advanced adenomatous polyps [13]. Also, cancer risk is directly related to the number of adenomas, as shown by the very high incidence of carcinoma in patients with >100 polyps such familial adenomatous polyposis [14].

1.2.2 Biology of colorectal cancer

The stepwise progression from normal to dysplastic epithelium and to carcinoma is earmarked by specific genetic alterations at known proto-oncogenes and tumor suppressor genes. This molecular pathway to colorectal cancer is triggered within a single cell that acquires a genetic alteration that provides it with a specific type of growth survival advantage. Loss of function mutations at the *APC* tumor suppressor gene on chromosome 5q21 occur in over 80% of colon adenocarcinomas [15], thus representing the earliest and rate-limiting genetic event in colorectal tumor initiation [16]. Indeed, *APC* mutations are present already at the ACF stage and they are related with the degree of dysplasia of these early lesions [17, 18]. It has been shown that *APC*'s main tumor suppressor activity resides in its capacity to regulate intracellular levels of β -catenin [19, 20, 21], a key member of the Wnt signal transduction pathway, which thanks to complex formation with the transcription factor TCF/LEF leads to transcriptional activation of target genes such as *c-Myc* and *Cyclin D*. Mutations of other members of the Wnt pathway, including β -catenin, Axin-1 and Conductin (Axin-2) have also been found in colorectal cancers [22, 23, 24]. The inactivation of both alleles of the *APC* gene can be detected in most of the intestinal tumors at early stages of development [16, 25],

in agreement with Knudson's two hit hypothesis [26]. However, *APC* second mutational hits are not randomly selected, but distributed according to the resulting levels of residual β -catenin down-regulating activity [27, 28]. In the situation in which a germline mutation is inherited or spontaneously occurred as in the FAP syndrome, the rate of initiation of colonic polyps is dramatically increased with the development of thousands of colorectal adenomas and the inevitable progression of some of these into carcinoma, unless the intestine is not surgically resected.

Activation of the *KRAS* oncogene represents the second step in the evolution towards colorectal cancer. The proto-oncogene *KRAS* encodes a 21 kDa protein that binds guanine nucleotides and is localized on the inner cell membrane. The identification of *KRAS* mutations has been the first major breakthrough in the molecular genetic analysis of colorectal cancer [29]. *KRAS* mutations are found in at least 50% of colorectal adenomas larger than 1 cm and in carcinomas but are infrequent in adenomas smaller than 1 cm in size [30], indicating a role in adenoma progression rather than initiation. Alternatively, mutations in other oncogenes like *BRAF* encoding for members of the same RAS pathway, are often found among adenomas [31]. *KRAS* mutations affect only specific codons (12, 13, 59-61) relevant for the endogenous guanine triphosphatase activity, leading to the constitutive activation of the Ras/Raf/MEK/ERK signal transduction pathway. Activation of this signaling pathway results in the transduction, from the surface receptors (such as epidermal growth factor receptor, EGFR), to the nucleus of signals for the transcriptional activation of target genes involved in cell proliferation and apoptosis inhibition like *Cyclin-dependent kinases*, *Cyclins* and *Bcl-2* [32] and thus malignant transformation.

Further malignant progression is accompanied by loss of all or part of the long arm of chromosome 18 (18q). At least 50% of large adenomas and 75% of carcinomas show loss of heterozygosity (LOH) at chromosome 18q [30, 33, 34]. The first candidate tumor suppressor gene in this chromosomal interval, the "deleted in colorectal cancer" gene (*DCC*), has been identified as a component of a receptor complex that mediates axon guidance in neurons [35]. However *DCC* mutations are rarely found in colorectal cancers [36].

Other tumor suppressor genes have been subsequently identified in this region and, among others, two intracellular mediators of the TGF- β signal transduction pathway *SMAD2* and *SMAD4*. Binding of TGF- β to the TGFBR2 receptor promotes the formation of heterodimer with the TGFBR1 receptor and phosphorylation of members of the SMAD family of intracellular mediators like *SMAD2*. Activated *SMAD2* binds *SMAD4* with its consequent nuclear translocation where the complex activates the transcription of genes responsible for a broad spectrum of cellular functions such as cellular growth inhibition, apoptosis, differentiation, and matrix production [37, 38]. Thus, when *SMAD2* or *SMAD4* are mutated, TGF- β signal is not transduced into the nucleus of the cell.

TGFBR2 mutations are also frequently found to affect TGF- β signaling in CRC. Overall, there is convincing mutational evidence for the major role of TGF- β pathway inactivation in the adenoma-to-carcinoma transition and, more in general, as primary tumor suppressor in human colorectal carcinogenesis.

Most malignant colorectal tumors are also characterized by loss of the short arm of chromosome 17 (17p). LOH or cytogenetic alterations at this locus correlate with the transition from benign adenoma to invasive cancer [30, 39, 40]. The *TP53* gene, encoding for p53, maps to this chromosomal interval. p53 is a multifunctional protein essential to cell growth control [41] often regarded to as the "guardian of the genome" due to his ability to block cell proliferation via transcriptional activation of cell cycle inhibitors, like p21, in the presence of DNA damage [42]. p53 also promotes apoptosis via transcriptional activation of genes such as *BAX* in situations where the DNA repair machinery cannot cope with the DNA damage load [43]. p53 alterations, often measured as aberrant overexpression in immunohistochemical assays, by direct DNA sequencing or by 17p allelic loss, have been reported in 4-26% of adenomas, approximately 50% of in situ carcinomas, and in 50-75% of adenocarcinoma [44, 45, 46, 47, 48]. The latter is indicative of the central role of loss of p53 function in the adenoma to carcinoma transition.

Figure 1.2.2 summarizes the accumulation of gene alterations in different pathways involved the CCR pathogenesis starting from normal epithelium.

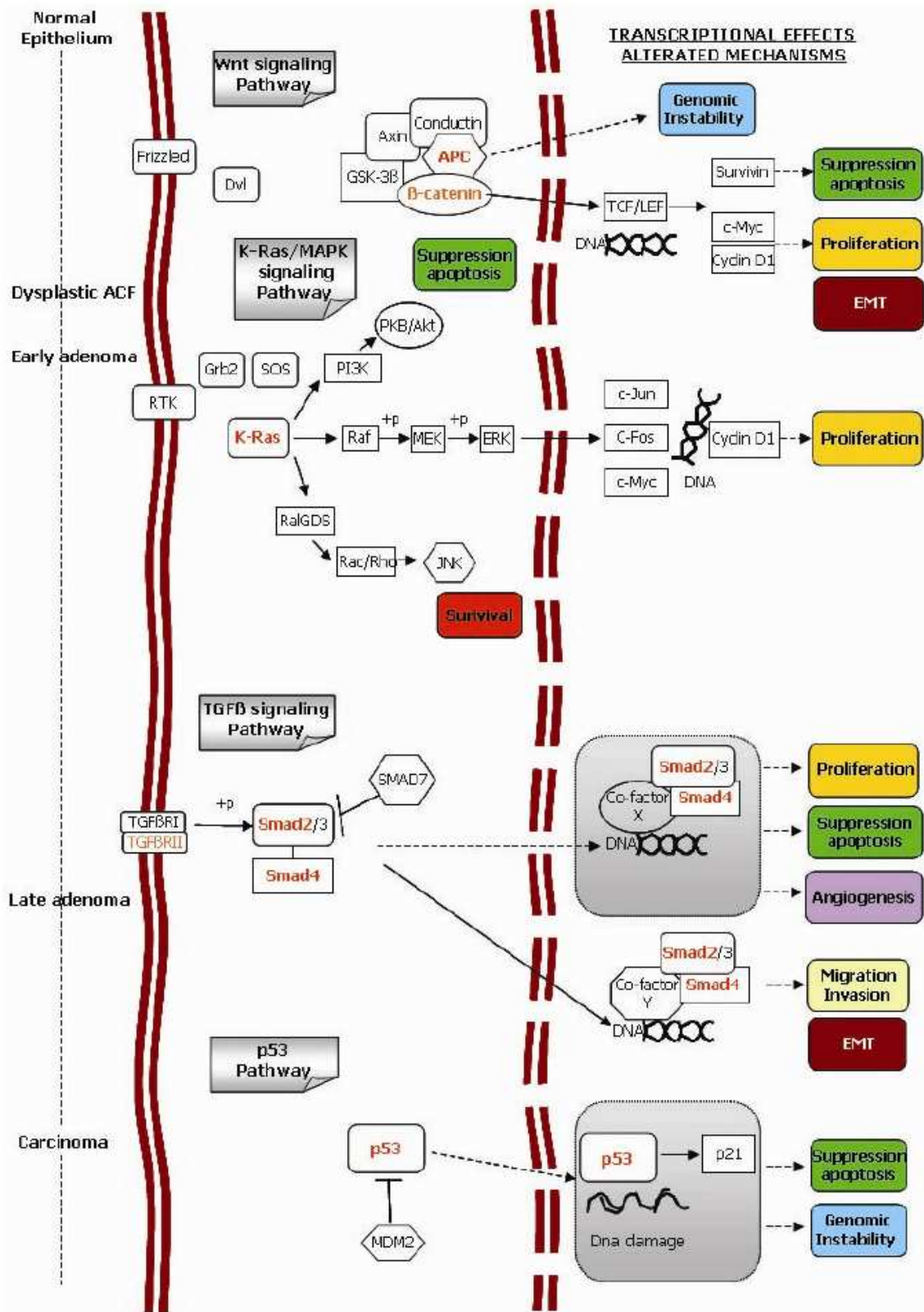


Figure 1.2.2: Schematic representation of the accumulation of alterations in different pathways along the adenoma-carcinoma sequence. In red are shown the genes frequently mutated in CRC. The different cellular alterations resulting from the accumulations of these signaling defects are listed in the right column. EMT, epithelial to mesenchymal transitions, contributes to local invasion and distant cancer metastasis.

Two main types of genetic instability (essential condition for tumors to develop and progress towards more malignant stages) have also been recognized in human CRC, they consist in microsatellite instability (MSI) and chromosomal instability (CIN) [49]. MSI results from loss of mismatch repair (MMR) function and is earmarked by tumor-specific frame-shift mutations in stretches of short repetitive DNA sequences (microsatellite repeats) distributed throughout the genome [50, 51]. Somatic defects in the same MMR genes well known in the autosomal dominant predisposition to CRC, HNPCC, are also found in approximately 15% of sporadic colon cancers. The vast majority of CRCs are characterized by abnormal chromosomal contents with a heterogeneous and broad spectrum of both numerical and structural changes such as inversions, deletions, duplications and translocations [52]. CIN, instead, may provide additional growth advantage to the cancer cell by accelerating the rate of LOH at tumor suppressor loci and/or by amplifying chromosomal regions encompassing oncogenes. Over 90% of all CRCs show chromosomal aberrations, some of which are recurrent and represent key chromosomal changes underlying colorectal cancer initiation and progression.

Also, epigenetic alterations such as DNA methylation and histone acetylation play an essential role in CRC progression. In fact, DNA methylation and thus inactivation of suppressor genes such as *MLH1*, *p14* (upstream inducer of the p53 tumor suppressor pathway) and *p16* occur in approximately 25-35% of colorectal cancers [53, 54]. Histone deacetylases (HDACs) instead are crucial regulating enzymes of histone acetylation, a phenomenon that is generally associated with transcriptional activation. Increased expression of HDACs in CRC has been demonstrated from several studies [55, 56] suggesting a physiological role in maintaining cell proliferation, survival and inhibiting differentiation.

The identification of stepwise acquisition of specific mutations in colorectal cancer has provided important clues relative to the cellular processes underlying tumorigenesis in the gastro-intestinal tract and has opened new avenues for tailor-made therapeutic approaches.

1.2.3 Colorectal cancer staging

Colorectal cancer staging is related to the depth of tumor penetration into the bowel wall and the presence of both regional lymph node involvement and distant metastases. These variables are incorporated into the staging system introduced by Dukes [57] and applied to a TNM classification method [American Joint Committee on Cancer (AJCC)], in which T represents the depth of tumor penetration, N the presence of lymph node involvement, and M the presence or absence of distant metastases (Figure 1.2.3). Superficial lesions that do not involve regional lymph nodes and do not

penetrate through the submucosa (T_1) or the *muscularis* (T_2) are designated as *stage I* ($T_{1-2}N_0M_0$) disease; tumors that penetrate through the *muscularis* but have not spread to lymph nodes are *stage II* disease ($T_3N_0M_0$); regional lymph node involvement defines *stage III* ($T_xN_1M_0$) disease; and metastatic spread to sites such as liver, lung, or bone indicates *stage IV* ($T_xN_xM_1$) disease. It results clear that a proper staging of CRC is important for subsequent therapeutic assessment.

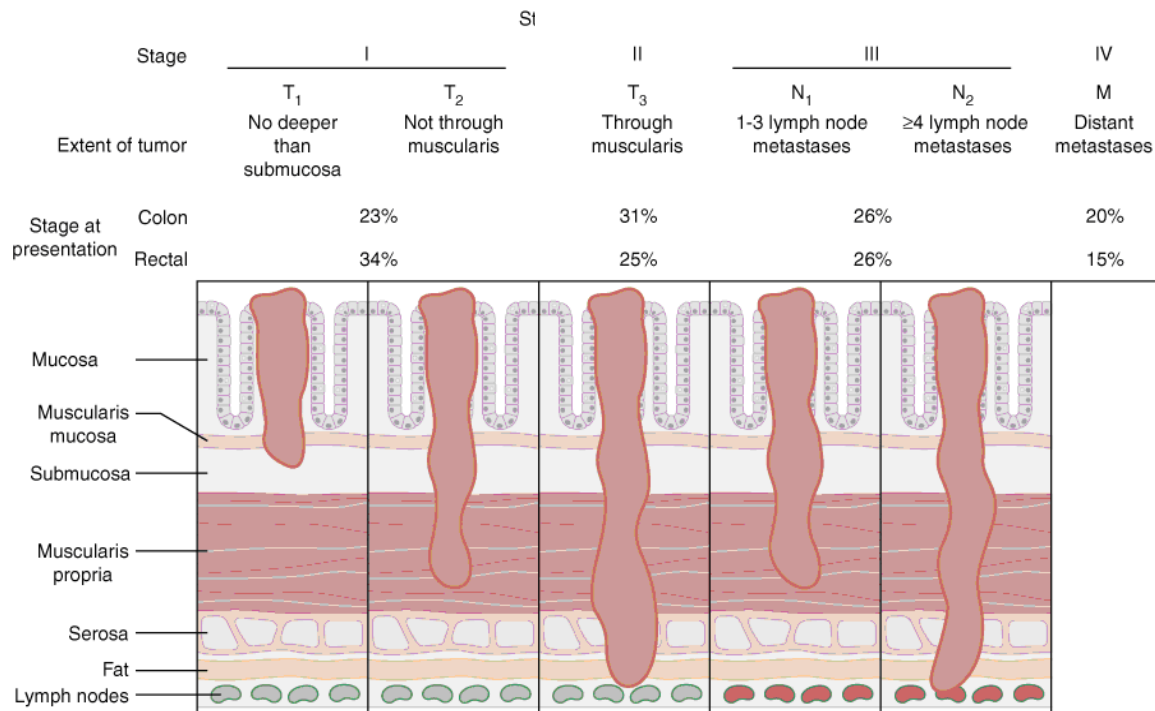


Figure 1.2.3: Staging of colorectal cancer. Figure has been reproduced from [58]

1.2.4 CRC treatment

Colorectal cancer therapy approach is closely related to the stage of the disease. Presently, the main therapy approaches for patients with CRC are surgery, radiation therapy, chemotherapy and targeted therapies (e.g. monoclonal antibodies). Depending on the stage of cancer, two or more of these types of treatment may be combined at the same time or used after one another.

Surgical resection remains the cornerstone of curative management of colorectal cancer [59], while radiation therapy is most effective as additional or adjuvant therapy either before or after surgery as it is shown to reduce the chance of cancer spread or recurrence [60]. Chemotherapy instead, represents the basis of metastatic CRC (mCRC) patients' therapy as approximately 50% of the patients with CRC develop metastases, and most probably die for the disease [61].

The goals of chemotherapy of mCRC include palliation of symptoms, prolongation of life, and, in selected cases of liver-only metastases, tumor regression to facilitate surgical resection of these metastases. Thanks to multiagent systemic therapy the median survival of a patient who has mCRC has improved during the last decade from less than 6 months to approximately 2 years [62, 63, 64].

5-FU, often modified by leucovorin (LV), has been clinically used for half a century [65] as a standard agent for mCRC. It was the only available agent until 1996, when irinotecan was approved. Over the last decade, oxaliplatin, capecitabine, bevacizumab, cetuximab, and most recently panitumumab have also been approved by the US Food and Drug Administration (FDA).

5-FU is inactive in its parent form and is converted within the cell to the cytotoxic metabolite fluorodeoxyuridine monophosphate (FdUMP). FdUMP forms a ternary complex with the reduced folate 5,10-methylenetetrahydrofolate and the enzyme thymidylate synthase (TS), which then leads to TS enzyme inhibition and subsequent inhibition of DNA synthesis and DNA repair. 5-FU can also be falsely incorporated into RNA and DNA, which leads to inhibition of mRNA translation and protein synthesis as well as inhibition of DNA synthesis and function, respectively.

LV (folinic acid) administration increases the intracellular pool of key reduced folates, specifically 5,10-methylenetetrahydrofolate, and stabilizes FdUMP and TS in a ternary complex and leads to optimal inhibition of the TS enzyme. To date, LV has been the most successful biomodulatory agent to be combined with 5-FU.

Capecitabine is an oral fluoropyrimidine with a similar mechanism of action and similar efficacy as 5-FU. Irinotecan is a derivative of camptothecin, found in *Camptotheca acuminata* (plant native to China) that inhibits DNA topoisomerase I and induces single-strand DNA breaks and replication arrest. Oxaliplatin is a third-generation platinum analogue that inhibits DNA replication and transcription by forming inter- and intra-strand DNA adducts/cross-links and induces apoptotic cell death.

Both LV (FOL, folinic acid) and 5-FU (F, fluorouracil) can be combined with irinotecan (IRI) or oxaliplatin (OX) with the treatment acronyms FOLFIRI or FOLFOX, respectively. These alternative treatments consist of administration of a bolus of 5-FU, LV, and either oxaliplatin or irinotecan and are shown to have similar efficacy [66, 67]. Either FOLFOX or FOLFIRI are therefore considered standard options for first-line treatment of mCRC. These regimens are typically given with bevacizumab, which is an example of target therapy together with cetuximab and panitumumab. Bevacizumab is a monoclonal antibody that binds to vascular endothelial growth factor (VEGF) ligand to inhibit angiogenesis. Its antineoplastic effect is ascribed to regression of microvascular density, inhibition of neovascularization, and normalization of grossly abnormal

tumor vasculature that permits more effective chemotherapy delivery to the tumor thus improving progression-free survival for mCRC patients [68].

Cetuximab and panitumumab therapy target, in mCRC treatment, is represented by EGFR (for details on EGFR and its role in cancer see Chapters 1.3 and 1.4). Both drugs are monoclonal antibodies (respectively chimeric human/mouse and fully humanised) able to inhibit ligand binding to the receptor and have been approved from FDA for the treatment of mCRC that has progressed on or following 5-FU, oxaliplatin, and irinotecan-containing regimens [69, 70, 71].

1.3 EPIDERMAL GROWTH FACTOR RECEPTOR

The epidermal growth factor receptor (EGFR/Her1/ErbB1) is a type I transmembrane receptor tyrosine kinase and a member of the ErbB receptor family. This family includes three other members: ErbB2 (Her2/Neu), ErbB3 (Her3), and ErbB4 (Her4). The 11 ligands currently identified for these receptors include epidermal growth factor (EGF), transforming growth factor alpha (TGF- α), HB-EGF (heparin binding EGF), betacellulin (BTC), amphiregulin (AR), epiregulin (EPR), epigen and the neuregulins (NRGs) 1-4 [72]. The exception is ErbB2 for which no natural ligand has yet been discovered.

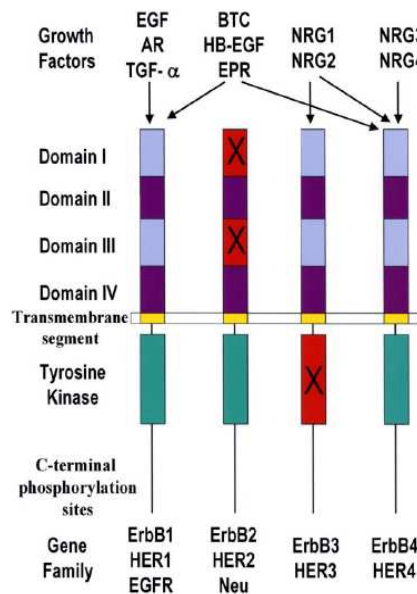


Figure 1.3: Epidermal growth factor family of ligands and the ErbB family. The inactive ligand-binding domains of ErbB2 and the inactive kinase domain of ErbB3 are denoted with an X.

On ligand binding, EGFR can either undergo receptor dimerization by binding to a second EGFR molecule or preferentially form a heterodimer with other members of the ErbB family, with the greatest affinity to ErbB2 [73]. However, it does not appear that ErbB2 homodimerizes at physiological expression levels, and homodimerization of ErbB3 receptors would not lead to receptor phosphorylation since ErbB3 is kinase inactive and thus must be trans-activated by heterodimerization with other ErbB receptors. The receptor dimerization subsequently mediates the activation of a complex signaling network that regulates cell growth, proliferation, survival, invasion and migration, and even angiogenesis [74].

1.3.1 Biochemical and structural characterisation of EGFR

EGFR is a 170 kDa protein that is heavily N-glycosylated [75], with carbohydrate accounting for ~20% of the molecular mass. The EGFR extracellular region is divided into four domains, numbered I-IV (Figure 1.3.1-1). Domains I and III (DI and DIII), also designated L1 and L2, are members of the leucine rich repeat family and are similar to domains found in the insulin receptor family [76]. Prior to receptor crystallization, it was known that both DI and DIII contribute to ligand binding [77]. Domains II and IV (DII and DIV), or the cysteine-rich (CR) domains, contain multiple small disulfide-bonded modules similar to those in laminin [78].

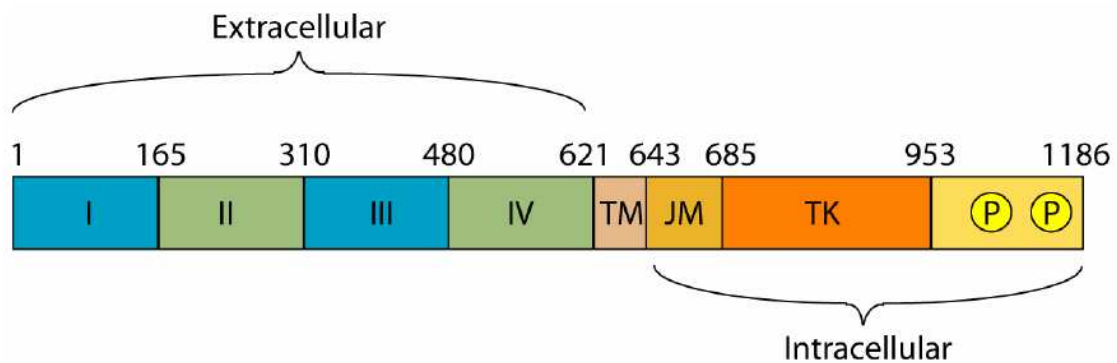


Figure 1.3.1-1: Schematic representation of EGFR domains. The extracellular region consists of domains I-IV, followed by a transmembrane region (TM) and the intracellular portion including the juxtamembrane domain (JM), the tyrosine kinase domain (TK), and the C-terminal tail containing tyrosine residues which become phosphorylated upon receptor activation.

The EGFR ectodomain has been crystallized in both monomer and dimer forms. The monomer exists in a tethered, closed, or autoinhibited state [79], with DII and DIV forming a tether contact (Figure 1.3.1-2, left). However, in the dimer structures of EGFR bound to EGF [80] or TGF- α [81], the receptor is in an untethered, open, or extended conformation, with ligand binding between DI and DIII (Figure 1.3.1-2, right). Although most cytokine receptors dimerize through ligand bridging the two receptor monomers [82], all dimerization contacts in the EGFR dimer are fully receptor-mediated. The dimer exists in a 2:2 receptor to ligand ratio, with multiple contacts through the DII dimerization arm (residues 242-259). An additional DII loop, residues 271-283, also contributes to important dimer contacts [83]. The dimerization interface may include DIV; however, in the dimer structures, DIV is either unresolved [80] or was not present in the crystallized protein [81]. Peptides mimicking portions of DIV can inhibit EGFR heterodimerization with Her3 [84], and

DIV mutations can impair the ability of ligand to bind and induce EGFR phosphorylation [85]. However, these potential DIV contacts contribute <9% of the free energy of dimerization as demonstrated by studies on soluble EGFR dimer formation [83]. For illustrative purposes, DIV has been added to the dimer structure in Figure 1.3.1-2 in the same relative orientation to DIII as seen in the tethered monomer. A low-resolution molecular envelope structure of the full EGFR dimer in solution has been obtained from small-angle X-ray scattering (SAXS), and it is consistent with this dimer structure [86].

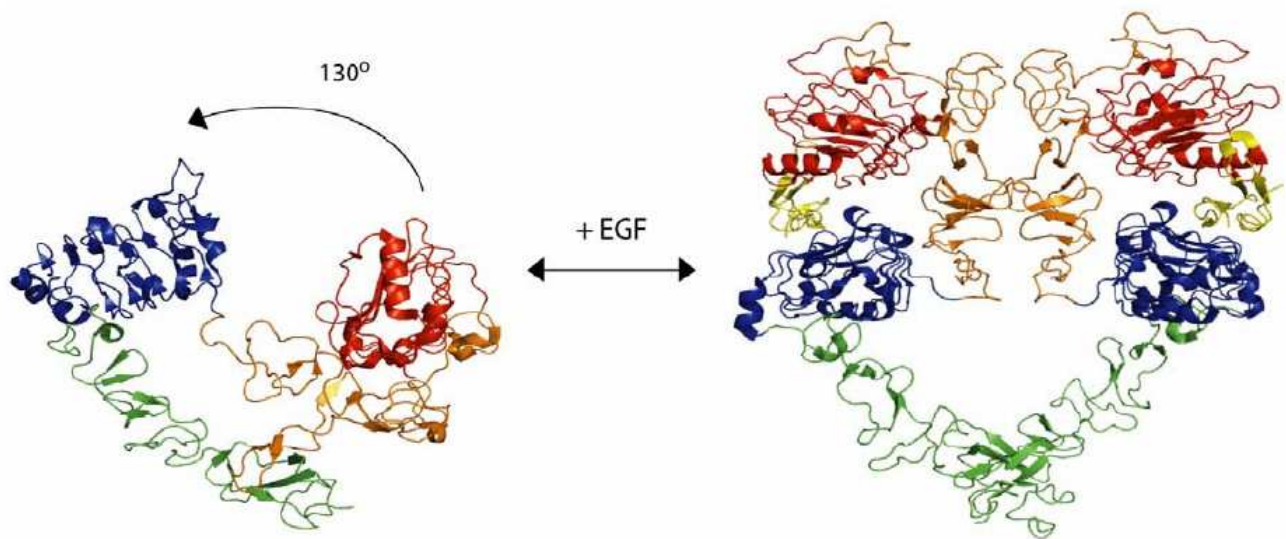


Figure 1.3.1-2: Crystal structures of monomeric and dimeric EGFR. Left) autoinhibited EGFR monomer, with domain I (DI), red; DII, orange; DIII, blue; DIV, green. A 130° rotation of DI and DII allows DI and DIII to come together to bind EGF ligand. Right) dimeric EGFR bound to EGF ligand in yellow. DIV is not resolved in this structure, but has been added in the same relative orientation to DIII as seen in the monomer. Figure has been reproduced from [87].

From the crystal structures of the monomer and dimer, a model for EGFR activation has been proposed [87]. In this model, the monomer mostly exists in a tethered conformation, in which the DII dimerization arm and other residues are obscured, thus preventing receptor dimerization. The monomer equilibrates between the tethered conformation and an extended conformation similar to that seen in the dimer. The binding of ligand between DI and DIII stabilizes the extended conformation, which exposes the DII dimerization arm and other residues, thus allowing the formation of the dimer. However, the breaking of the tether is necessary but not sufficient for dimer formation, as demonstrated through mutations and deletions of DIV [81, 88, 89]. It also appears that certain types of receptor glycosylation can shift the equilibrium toward the extended form [90, 91]. It has subsequently been found that the DII-DIV tether interaction is not necessarily responsible for

maintaining the receptor in the autoinhibited conformation; in fact, mutating every tether interaction in soluble EGFR still leads to an autoinhibited conformation [86]. In addition, it appears that ligand binding is necessary to stabilize the conformation of the DII loop 271-283, which is an important dimerization contact [83].

EGFR has a single transmembrane domain, and the intracellular portion contains a short juxtamembrane region, the tyrosine kinase, and a C-terminal tail containing tyrosine residues which become phosphorylated upon receptor activation (Figure 1.3.1). The EGFR kinase domain has been independently crystallized, revealing an intrinsically autoinhibited domain resembling Src and cyclin-dependent kinases (CDKs) [92]. In contrast to most kinases, phosphorylation of the EGFR activation loop is not necessary for its activation [93]. Instead, the EGFR kinase is activated by an asymmetric dimer in which the C-terminal lobe of one kinase domain binds to the second kinase domain in a manner analogous to cyclin in activated CDK/cyclin complexes. Thus, ligand binding brings two receptor monomers together and allows for the dimerization and subsequent activation of the kinase domains. The extent of EGFR kinase activation depends on the effective local concentration of the receptor, since the probability of dimerization will increase with increasing kinase domain density as experimentally demonstrated using increasing concentrations of EGFR kinase domains tethered to the vesicles surface [92].

1.3.2 EGFR: Signaling and trafficking

The receptor dimerization event allows for kinase activation and trans-phosphorylation of residues in the intracellular domain of EGFR. The phosphorylated tyrosine residues and the surrounding amino acids are specifically tailored to interact with a unique collection of second messengers such that, depending on the stimulating ligand and dimerization partner, a specific biological response may be precisely induced [72]. Following stimulation of EGFR by EGF, the major sites of phosphorylation include tyrosines 1068, 1148, 1173 [94]. These phosphorylated tyrosines serve as specific binding sites for several adaptor proteins, such as phospholipase C γ , CBL, GRB2, SHC and p85, mainly characterized by the presence of the phosphotyrosine binding domain (PTB), SH3 domains that recognize proline-rich sequences and SH2 domains (Src-homology 2). Many of these interactions have been characterized in detail, such as GRB2 binding to EGFR tyrosine 1068 and SHC binding to EGFR tyrosines 1148 and 1173 [95, 96]. Several signal transducers then bind to these adaptors to initiate multiple signaling pathways, including mitogen-activated protein kinase (MAPK), phosphatidylinositol 3-kinase (PI3K) /AKT and the signal transducer and activator of transcription (STAT) pathways [97].

As mentioned earlier, KRAS protein is a pivotal downstream component of the EGFR signaling cascade able to activate the Ras/Raf/MEK/ERK pathway, which mediates cell growth and cell cycle entry via phosphorylation of key transcription factors (c-FOS and MYC) of target genes like *Cyclin-dependent kinases* and *Cyclins* [17]. The PI3K signaling cascade, instead, plays an integral role in regulating several key cellular processes including cell survival and growth, proliferation, cell migration and angiogenesis [98]. The most relevant effector of PI3K for cell proliferation and survival is the serine/threonine kinase Akt. Activation of Akt leads to enhanced cell growth and proliferation through downregulation of p21 and p27 cell cycle inhibitors, through increased translation and stabilization of cyclin D1, while the process of cell survival is mediated through several different mechanisms, including inhibition of the pro-apoptotic Bcl-2 family member Bad [99]. The third EGFR downstream pathway is represented by STAT proteins, latent cytoplasmic transcription factors able to convey signals from growth-factor receptors to the nucleus. Homo- and heterodimerization of STAT proteins is a prerequisite for activation and translocation to the nucleus, and is mediated by tyrosine phosphorylation of critical residues. EGFR activation results in STAT dimers activation that play a crucial role in fundamental biological processes such as cell proliferation, apoptosis and angiogenesis, thus finding place in a pivotal position for tumorigenesis [100]. It is important to note that STAT regulation of genes that control cell proliferation and survival varies among different tumour types [101,102] due to cell-type specific differences in STAT-interacting proteins, such as other transcription factors [103, 104].

In addition, EGFR can be trans-activated by other proteins, such as G-protein-coupled receptors (GPCRs) [105]. The various signaling cascades associated with EGFR activation are summarized in Figure 1.3.2-1. It has also been observed that activated EGFR may undergo nuclear translocation and subsequently regulate gene expression: in fact chromatin immunoprecipitation studies demonstrated that EGFR is associated with the promoter region of cyclin D1 gene [106].

The activation of EGFR thus leads to multiple cell responses, including cellular growth, differentiation, and migration.

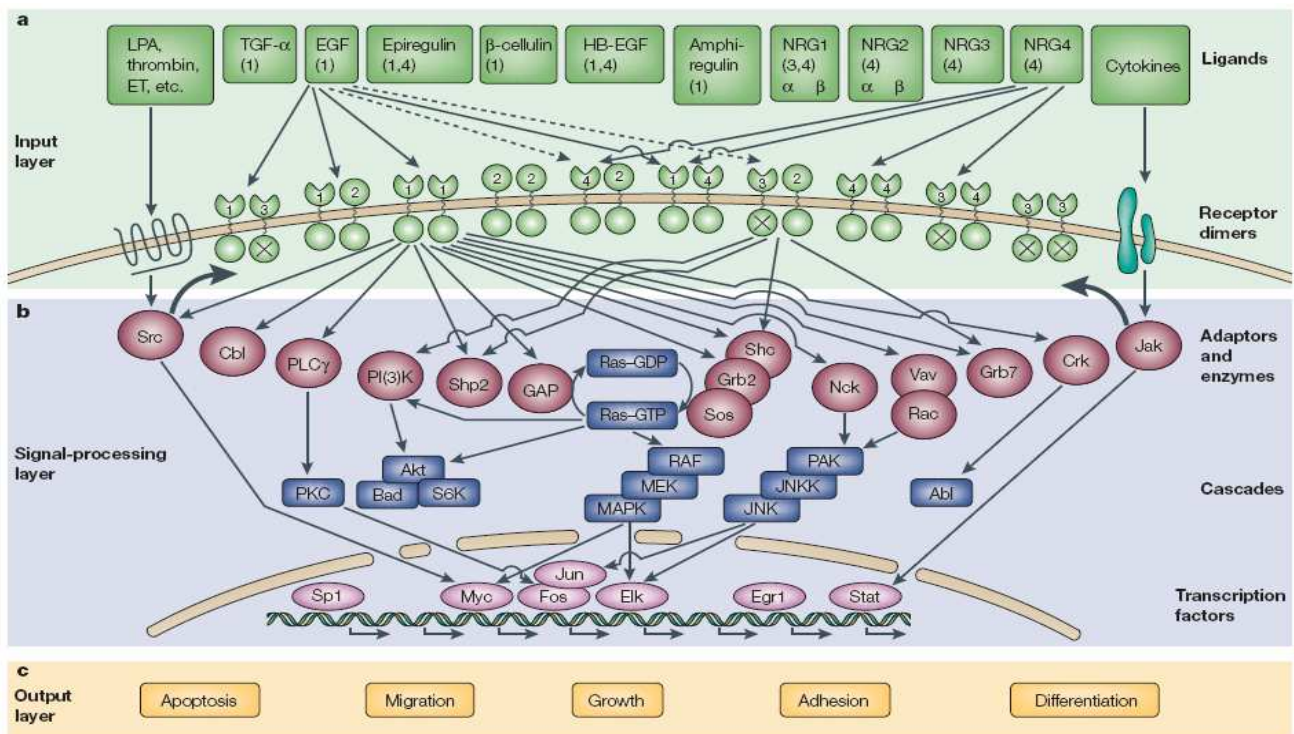


Figure 1.3.2-1: EGFR signaling network. **a)** EGFR family ligands are shown with their binding specificities, other ligand specificities are shown in parentheses. **b)** Signaling to the adaptor protein/kinase layer. **c)** Possible cellular outcomes based on EGFR signaling. Figure has been reproduced from [106].

In the absence of ligand, EGFR is constitutively internalized with a half life of ~30 minutes and quickly recycled back to the cell surface, leading to a total receptor distribution of ~80-90% on the cell surface at any given time (Figure 1.3.2-2) [107]. The metabolic half-life of EGFR in a tumor cell line is 20 hours [108]; thus, a single receptor will cycle through the endocytic pathway many times during its lifetime. Ligand activation increases the rate of EGFR endocytosis 5-10 fold [109]. In addition, activated EGFR dimers bound to EGF are preferentially retained in the endosomes and not recycled [110], and these endosomes mature into multivesicular bodies and are targeted to lysosomes [111]. This leads to the specific degradation of activated receptors and overall receptor downregulation. Earlier reports indicated that ligand-accelerated internalization required EGFR kinase activity [112, 113], but a recent study found that receptor dimerization was sufficient to induce rapid internalization and that kinase activity was unnecessary [114]. Although receptor ubiquitination does not affect EGFR internalization rates [115, 116], ubiquitination by c-Cbl targets receptors to the lysosome and is dependent on kinase activity and an intact C-terminal region [117]. While receptor internalization has often been viewed as a means of signaling attenuation, it has been shown that activated EGFR continues to signal while in the endosome through certain signaling pathways [118, 119]. Mathematical modelling and experiments have also demonstrated that ErbB2, often described as the preferred heterodimerization partner for ErbB receptors [73],

reduces the rate of internalization and increases the fraction of recycled EGFR/Her2 heterodimers [120].

For its importance EGFR trafficking has been the subject of much mathematical modelling, and the system serves as a paradigm for other ligand-binding receptors [108, 121, 122].

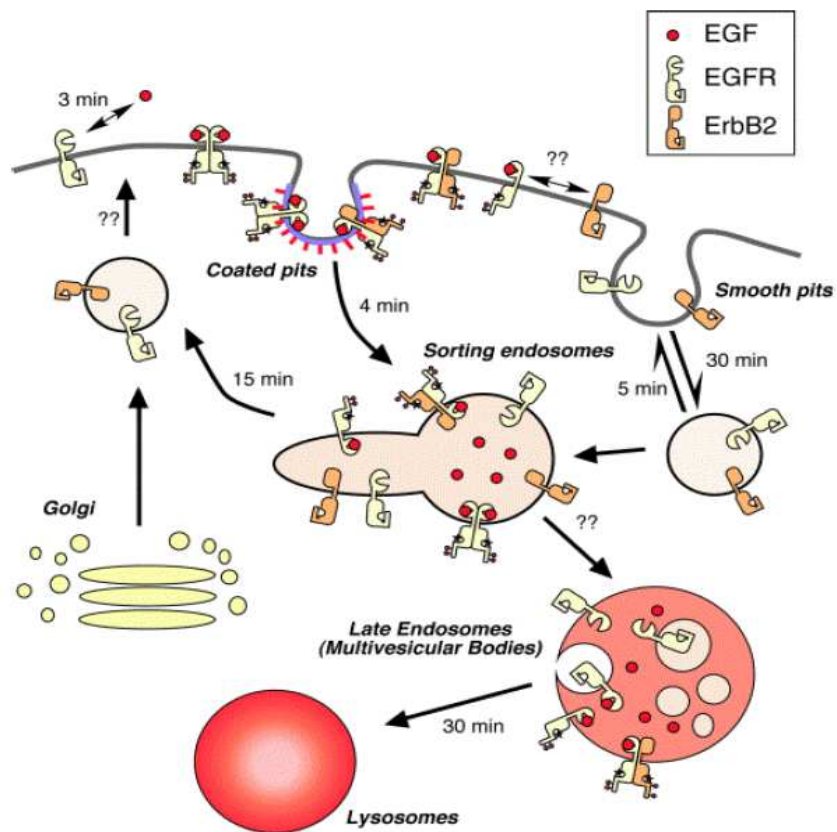


Figure 1.3.2-2: EGFR intracellular trafficking. Activated EGFR homo- and heterodimers are internalized through clathrin-coated pits and preferentially degraded. Approximate mean time of the processes are indicated. Figure has been reproduced from [108].

1.4 EGFR ROLE IN CANCER

EGFR was the first receptor to be directly linked to human cancer [123], and because EGFR activation often leads to cellular growth, its signaling can provide tumor cells with substantial survival advantages. In addition, EGFR signaling has been implicated in tumor cell production of pro-angiogenic factors and cellular migration and invasion [124]. In fact, upstream of RAS, activation of EGF receptor has been shown to induce scattering of human cancer cells via tyrosine phosphorylation of β -catenin [125]. In particular, β -catenin tyrosine phosphorylation at residue 654 results in loss of cell-cell adhesion by disturbing the functionality of the adherens junction functionality through E-cadherin destabilization and loss of contact with the actin cytoskeleton [126]. These effects on cell-cell adhesion underlie epithelial to mesenchymal transitions (EMT) and are known to contribute to local invasion and distant cancer metastasis. EGFR dysregulation has been observed in a wide variety of carcinomas, including colorectal, head and neck, breast, bladder, and non-small-cell lung cancer (NSCLC) [105]. Excessive EGFR signaling can arise from receptor overexpression, autocrine signaling, or mutation. Normal cells usually express 4×10^4 to 1×10^5 EGF receptors per cell, but tumor cells can express as many as 2×10^6 [127]. Receptor overexpression commonly develops due to gene amplification, although it was quite recently reported that the hypoxic microenvironment of tumors can also induce overexpression of EGFR by increasing EGFR mRNA translation [128]. In CRC, 22-75% of tumors overexpress EGFR [129], and the observed percentages of tumors overexpressing EGFR in various types of cancer are listed in Table 1.4. Furthermore, elevated levels of EGFR serve as a prognostic indicator for poor survival rates [130].

Table 1.4: EGFR overexpression in different tumor types.

Tumor type	Percentage of tumors overexpressing EGFR
Colon	22-75%
Head and neck	80-100%
Pancreatic	30-50%
Non-small-cell lung	40-80%
Breast	14-91%
Renal	50-90%
Ovarian	35-70%
Glioma	40-63%
Bladder	31-48%

In addition, EGFR ligands can be overexpressed, resulting in high levels of autocrine signaling when the receptor is present [131]. Autocrine production of TGF- α or EGF is also associated with reduced cancer survival [132]. Various activating EGFR mutations have been observed in tumor samples. Mutations in the EGFR kinase domain, which are clustered around the ATP-binding pocket of the enzyme, have been observed in many types of carcinomas including ovarian, colorectal, and head and neck and NSCLC. Most of these mutations have been shown to hyperactivate the kinase and have oncogenic activity [133].

Finally, in addition to the full-length transmembrane forms of ErbB receptors, normal and malignant cells synthesize soluble ErbB isoforms (sErbBs) that lack the TMD and ICD of the receptor, as well as proteolytically truncated isoforms (tErbBs) that encompass only the TMD and/or ICD of the receptor [reviewed by 134] (Figure 1.4.1). Soluble ErbB isoforms have been identified for all four members of the ErbB family and can be generated either by alternate mRNA splicing/processing events or via proteolytic cleavage of the full-length receptor. This events result in 60-kDa, 80-kDa and 110-kDa sErbB1/sEGFR isoforms; 68-kDa, 100-kDa, 105-kDa and 110-kDa sErbB2 isoforms; 20-kDa, 45-kDa, 50-kDa, 76-kDa, and 85-kDa sErbB3 isoforms; and the 120-kDa isoform of sErbB4 (Figure 1.4.1) [134]. The natural occurrence of this soluble, truncated, and other alternate ErbB receptor isoforms produces yet another level of complexity on the regulation of EGFR signal transduction.

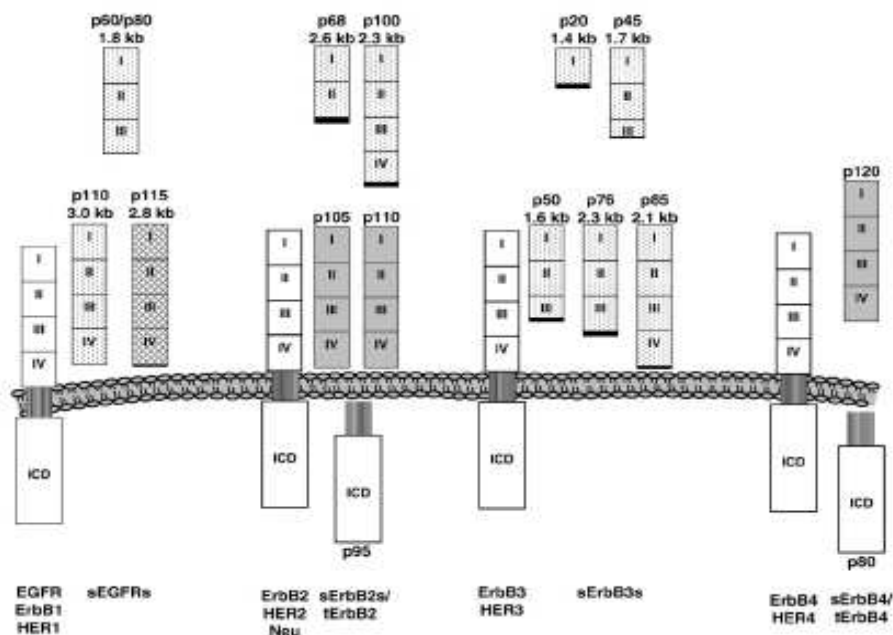


Figure 1.4.1: Schematic summary of full-length, soluble, truncated, and alternate human ErbB receptors. Gray boxes) sErbBs produced by proteolytic cleavage, dotted boxes) sErbBs produced by alternate transcripts, cross-hatched boxes) the only known “sErbB” resulting from an aberrant translocation event involving the EGFR gene. Figure has been reproduced from [134].

Because of the importance of EGFR family in cancer and in particular in CRC, EGFR is a promising target for rational oncology therapies designed to inhibit receptor signaling. Targeting the ErbB network may be achieved by inhibiting the tyrosine kinase (catalytic domain) with small molecules (TKIs) or by inhibiting the extracellular domain with monoclonal antibodies (Figure 1.4.2).

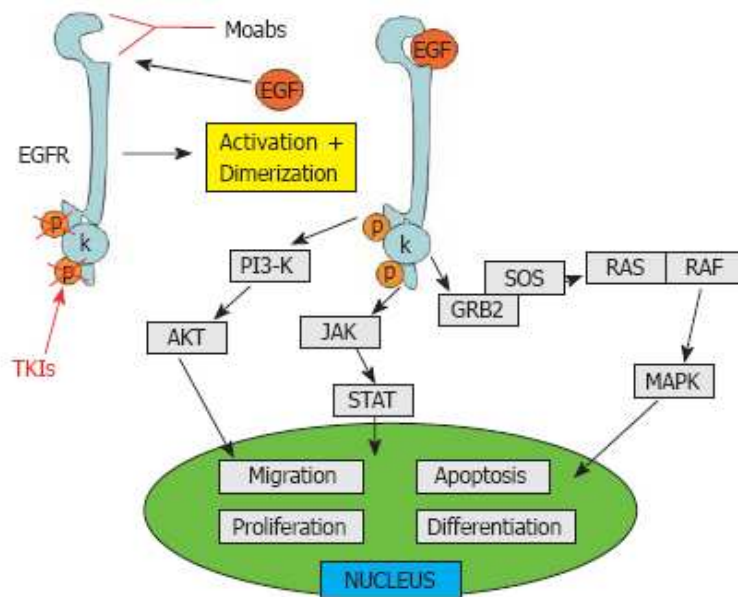


Figure 1.4.2: EGFR network and target therapies.

Gefitinib (Iressa, ZD1839; AstraZeneca) [135] and erlotinib (Tarceva, OSI-774; OSI/Genentech/Roche) [136] are two EGFR-targeted TKIs approved from the FDA for the treatment of mCRC, that inhibit receptor autophosphorylation and block downstream signal transduction. As previously described, monoclonal antibodies such as cetuximab (Erbix, IMC-C225; ImClone Systems) and panitumumab (Vectibix, ABX-EGF; Amgen/Abgenix) block the interaction between natural ligands and the EGF receptor in the extracellular space resulting in decreased tyrosine phosphorylation and reduced cell proliferation as well as increased rate of receptor internalization. Despite their promising effects in CRC, the forementioned EGFR target therapies have shown little activity, due to the established resistance mechanisms [137, 138], and elevated adverse events including diarrhoea, skin toxicity (including acne-like rash), neutropenia and asthenia that have been largely reported [61, 139].

1.5 AIM OF THE RESEARCH

EGFR abnormalities are associated with all aspects of carcinogenesis, cell proliferation, inhibition of apoptosis, angiogenesis and metastasis. Overexpression of EGFR has been reported in several tumor types, most notably colorectal (object of this study), head and neck, and lung cancers, where it typically correlates with poor clinical outcomes. Thus, interference with EGFR receptor activation and/or with its intracellular signal transduction pathways represents a promising strategy for the development of novel and selective anticancer therapies. To date, two strategies for therapeutic inhibition of EGFR are under clinical development for the treatment of CRC: monoclonal antibodies and TKIs. Although results seemed to be encouraging they have shown little activity, due to the established resistance mechanisms, and elevated cytotoxicity.

In this respect, shikonin is a naturally occurring naphthoquinone isolated from the roots of many traditional medicinal plants, that has been demonstrated to have great anti-tumor potential by inhibiting the cell growth of various cancer cell lines, inducing apoptosis in leukemia HL-60 cells and inhibiting EGFR signaling in human epidermoid carcinoma cells [140, 141]. Moreover, a shikonin derivative, β -hydroxyisovalerylshikonin, strongly inhibits EGFR kinase activity and inhibition results non-competitive with respect to ATP, suggesting that both it and the parent compound may bind to the peptide-binding site [142, 143].

In this thesis work, the anti-tumor activity and the efficacy of FR18, 2-(8-amino-octylamino)-[1,4]naphthoquinone, a molecule containing the same naphthoquinone core as shikonin, was tested as a novel EGFR inhibitor by using the human colon adenocarcinoma cell line, HT-29, as a cellular model. Flow cytometry, immunoprecipitation, western blot and confocal spectral microscopy analysis were performed in order to evaluate the biological effects induced by FR18 on HT29 cells, paying particular attention to the tyrosine kinase activity and to the ability of the epidermal growth factor receptor to bind its natural ligand, EGF.

Therefore, a second aspect of the research was focused on the investigation of the direct EGF/EGFR complex interaction which represents a challenging but important system that can lead to significant general knowledge about receptor-ligand interactions, and the design of new drugs intended to interfere with EGFR binding activity. EGF/EGFR interaction studies were performed by surface plasmon resonance (SPR) biosensor technique which allows the study of biomolecular interactions in real-time and label-free with a high degree of sensitivity and specificity.

2. TECHNIQUES

2.1 CONFOCAL LASER SCANNING MICROSCOPY

Laser scanning confocal microscopy (LSCM) is an invaluable tool for a wide range of investigations in the biological and medical science primarily because the technique enables visualization deep within both living and fixed cells and tissues and affords the ability to collect sharply defined optical sections from which three-dimensional renderings can be created.

The basic concept of confocal microscopy was originally developed by Marvin Minsky in the mid-1950s [144, 145]. During the late 1970s and the 1980s, advances in computer and laser technology, coupled to the application of a wide array of new synthetic and naturally occurring fluorochromes, led to a growing interest in confocal microscopy.

In epi-illumination scanning confocal microscopy systems, the laser light source and photomultiplier detectors are both separated from the specimen by the objective, which functions as a well-corrected condenser and objective combination. Light emitted by the laser system (excitation source) passes through a pinhole aperture that is situated in a conjugate plane (confocal) with a scanning point on the specimen and a second pinhole aperture positioned in front of the detector (a photomultiplier tube) as shown in Figure 2.1.1.

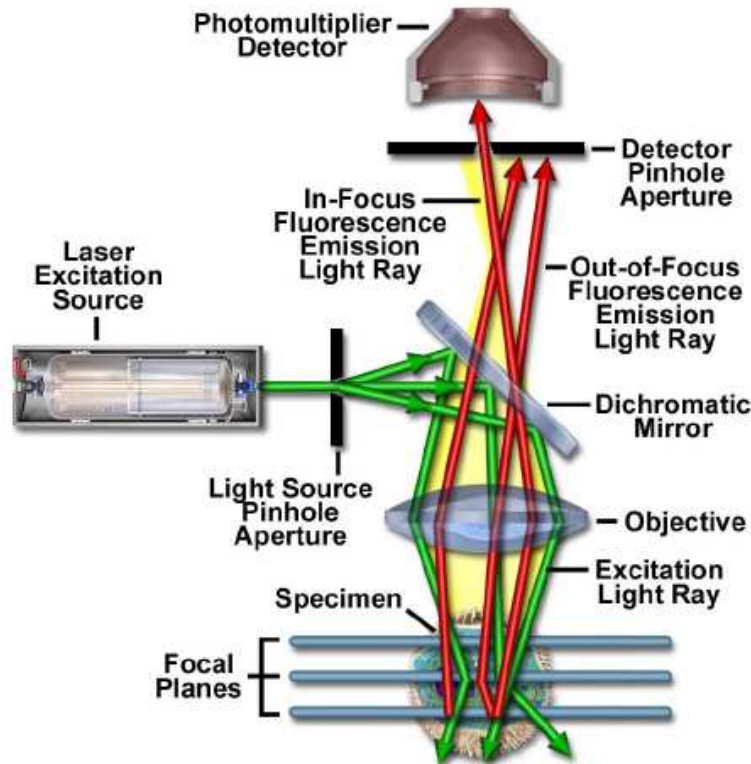


Figure 2.1.1: Optical pathway and principal components in an epi-illumination laser scanning confocal microscope.

As the laser is reflected by a dichromatic mirror and scanned across the specimen in a defined focal plane, secondary fluorescence emitted from points on the specimen (in the same focal plane) passes back through the dichromatic mirror and is focused as a confocal point at the detector pinhole aperture.

This optical configuration enables the following advantages: i) reduced image blur by scattered light, ii) increased resolution iii) improved signal-to-noise ratio, iv) the opportunity to clearly examine specimens in 3D.

In traditional wide-field epi-fluorescence microscopy, the entire specimen is subjected to intense illumination from an incoherent mercury or xenon arc-discharge lamp, and the resulting image of secondary fluorescence emission can be viewed directly in the eyepieces or projected onto the surface of an electronic array detector.

In contrast to this simple concept, the mechanism of image formation in a confocal microscope is fundamentally different. The significant amount of fluorescence emission that occurs at points above and below the objective focal plane and is not confocal with the pinhole is not detected by the photomultiplier and does not contribute to the resulting image. Refocusing the objective in a confocal microscope shifts the excitation and emission points on a specimen to a new plane that becomes confocal with the pinhole apertures of the light source and detector. The result is a set of optical sections that collected and summed along the z axis allows the reconstruction of specimen's 3D structure. Resolution along the z axis for a confocal microscope is given by:

$$z_{\min} = 2\lambda\eta/(\text{NA}^2)$$

where η is the medium refraction index, λ the wavelength and N.A. is the numerical aperture.

The confocal image of a specimen is reconstructed, point by point, from emission photon signals by the photomultiplier and accompanying electronics, yet never exists as a real image that can be observed through the microscope eyepieces.

BioRad MRC1024 UV and Nikon C1s confocal laser scanning microscopes were used in this thesis. BioRad MRC1024 UV system uses a two laser excitation: i) Argon ion UV laser (Coherent), emitting at 357 nm, 361 nm and 488 nm, powered with 100 mW, ii) Krypton/Argon ion visible laser (Bio-Rad), which emits at wavelengths of 488 nm, 568 nm and 647 nm and is powered with 15 mW. The two lasers are coupled to scan head through an optical fibre connection. The scan head (Figure 2.1.2) contains, in addition to the fluorescent filter sets, three photomultiplier tubes. The scanning is done by a galvanometer-based raster scanning mirror system.

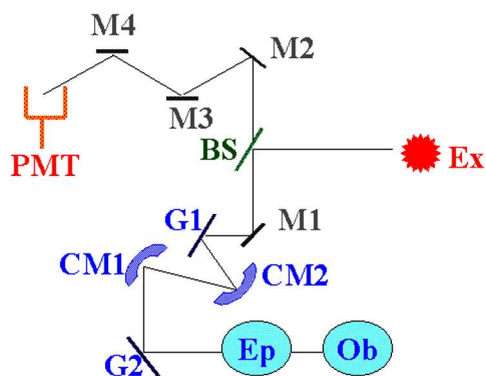


Figure 2.1.2: Diagram of the scanning head in Bio-Rad 1024 UV. Laser light (Ex) reflected by dichromic mirror (BS) is sent to the objective (Ob) through the M1 mirror, the G1 and G2 galvanometric mirrors and the CM1 and CM2 convex mirrors. Emitted fluorescence is sent to the photomultiplier (PMT) through the M2, M3 and M4 mirrors system.

The microscope used is the Nikon Eclipse TE300: an inverted microscope equipped for conventional light microscopy, fluorescence, reflection and phase contrast. Windows NT operating system is used together with LaserSharp 2000 acquisition software (Bio-Rad, Hercules, CA).

Nikon C1s instrument permits the acquisition of spectral imaging (also referred to as emission fingerprinting) followed by linear unmixing of emission profiles in specimens labeled with combinations of fluorescent proteins or fluorophores having overlapping spectra.

Nikon C1s uses a three laser excitation: i) BD laser, emitting at 405 nm, powered with 25 mW, ii) Argon ion laser, which emits at wavelengths of 488 nm and is powered with 10 mW, iii) R-HeNe laser emitting at 633 nm powered with 5mW. The lasers unit is coupled to the scan head through an optical fibre connection. As shown in Figure 2.1.3, the scanning head is coupled to a standard fluorescence detector which permits simultaneous 3-channel fluorescence imaging and a spectral detector able to acquire 32 channels of fluorescence spectra over a 400-750 nm wavelength range with a switchable wavelength resolution of 2.5 nm, 5 nm, or 10 nm.

Nikon Eclipse TE300 UV confocal microscope, equipped with a Nikon PlanApo 60 \times , 1.4-NA oil immersion lens is used and images are analyzed using the EZ-C1 software (Nikon).

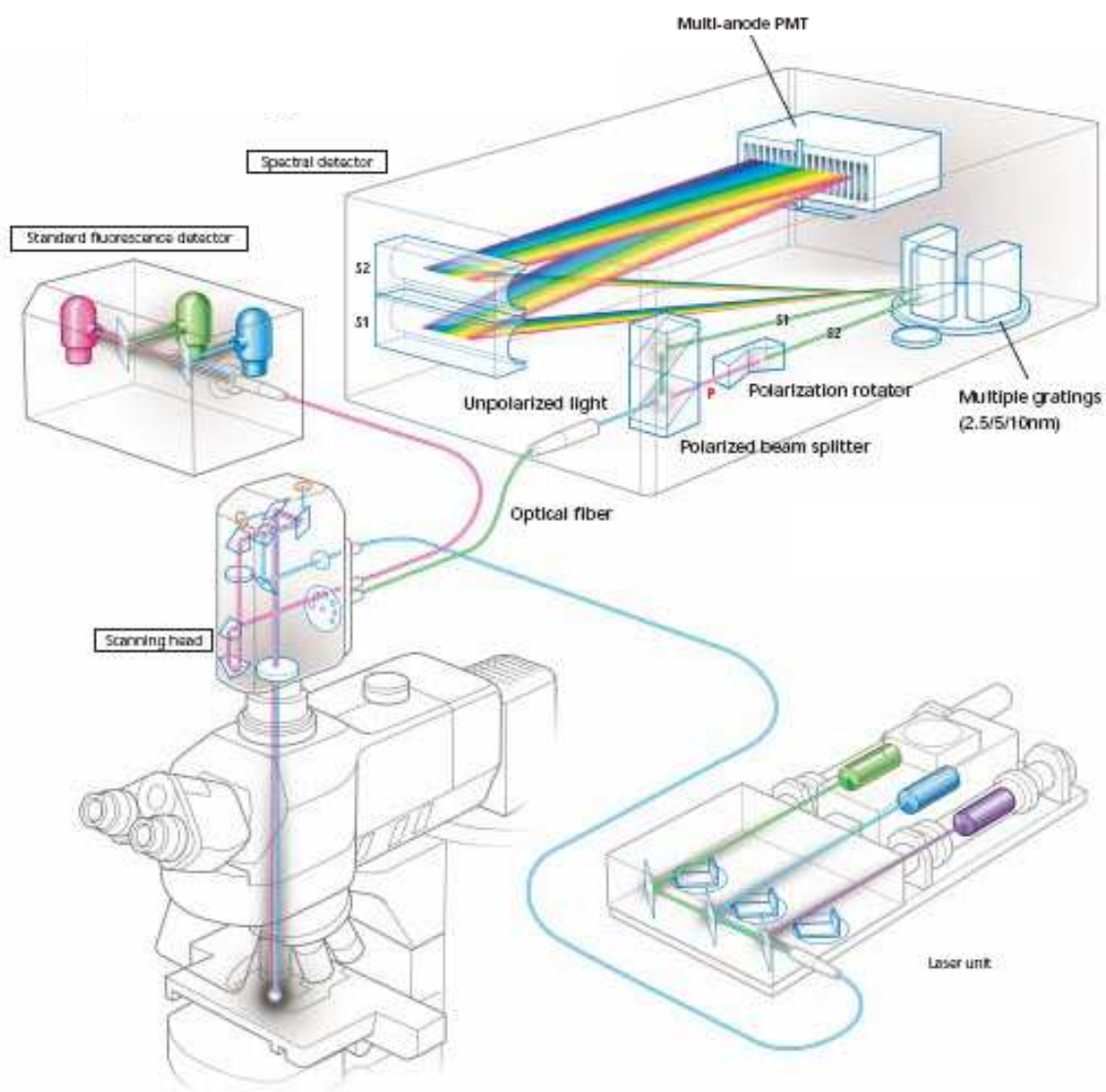


Figure 2.1.3: Schematic representation of Nikon C1s spectral imaging confocal laser microscope.

2.2 SURFACE PLASMON RESONANCE BIOSENSORS (BIACORE)

Biosensors are analytical devices comprised of a biological element (tissue, microorganism, organelle, cell receptor, enzyme, antibody) and a physico-chemical transducer. Specific interaction between the target analyte and the biological material produces a physico-chemical change detected by the transducer. The transducer then yields an analogical electronic signal proportional to the amount (concentration) of a specific analyte or group of analytes.

Surface Plasmon Resonance (SPR) biosensor technology is a label-free technology for monitoring biomolecular interactions as they occur [146]. The detection principle relies on SPR, an electron charge density wave phenomenon that arises at the surface of a metallic film when light is reflected at the film under specific conditions. The resonance is a result of energy being transformed from incident photons into surface plasmons, and is sensitive to the refractive index of the medium on the opposite side of the film from the reflected light.

When incident polarised light is passed through a higher refractive index material (glass) to a lower refractive index material (air), part of the light is reflected and part is refracted. When the angle of incident light is greater than a critical angle, total internal reflection occurs (TIR) and the electric field component of the light, also called evanescent wave, propagates and decays exponentially along the interface of the two media. If the TIR interface is coated with a noble metal (gold) film the photon energy of the evanescent wave is transferred to the free electrons within the gold film (plasmons) which excited give rise to an additional electric field. At a defined angle of incidence (resonance angle) the wave vectors of the plasmons and the evanescent field are coupled and surface plasmon resonance occurs. This resonance can be physically observed by the sudden drop in angle-dependent reflectance accompanied by energy loss (Figure 2.2.1). This is called the minimum of reflectance and is the typical data point recorded in experimentation. SPR-dip shift in time is measured in resonance units (RU).

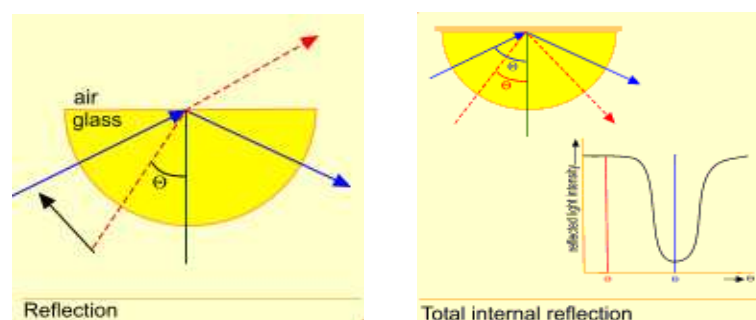


Figure 2.2.1: SPR is observed as a dip in the reflected light intensity at a specific angle of reflection.

Biacore (GE Healthcare, Uppsala, Sweden) has pioneered commercial SPR biosensors offering a unique technology for collecting high quality, information-rich data from biomolecular binding events. Biacore's optical biosensors (Figure 2.2.2) are designed around three core technologies:

1. An optical detector system that monitors the changes in SPR signal brought about by binding events in real time.
2. An exchangeable sensor chip consisting of a glass slide and a thin gold-film upon which one of the interacting biomolecules is immobilized or captured. The resulting biospecific surface is the site where biomolecular interactions occur.
3. A microfluidic and liquid handling system that precisely controls the flow of buffer and sample over the sensor surface.

These systems are contained within the processing unit that communicates with a computer equipped with control and data evaluation software.

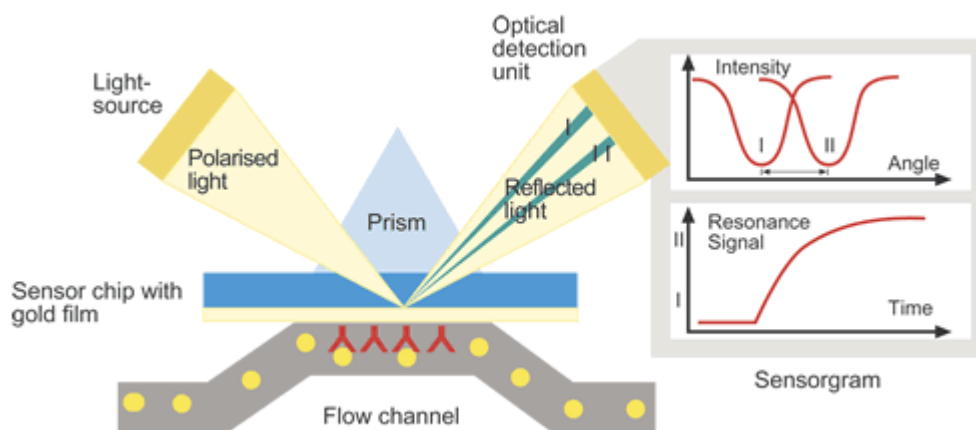


Figure 2.2.2: Schematic representation of SPR biosensors.

In the simplest case of an SPR measurement, a target component or analyte is captured by the capturing element or so-called ligand. The ligand is permanently immobilized on the sensor surface previous to the measurement. Molecules can be covalently linked to sensorchips with several binding techniques utilizing different intrinsic active groups in the ligands.

The most common coupling chemistries are showed in Figure 2.2.3.

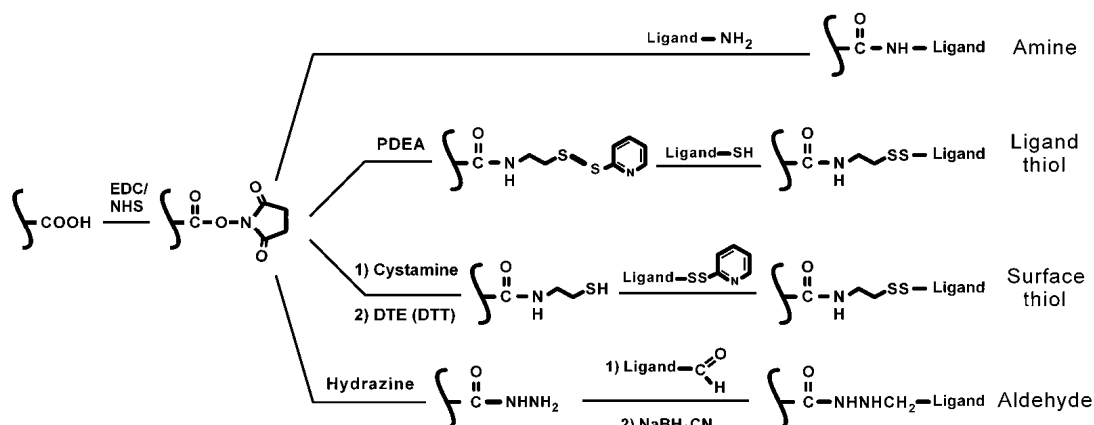


Figure 2.2.3: Common coupling chemistries applied to immobilize molecules on Biacore sensor chips.

The event of capturing the analyte by the ligand gives rise to a measurable signal called direct detection. Figure 2.2.4 shows the sensor signal step-by-step in the measurement cycle with direct detection.

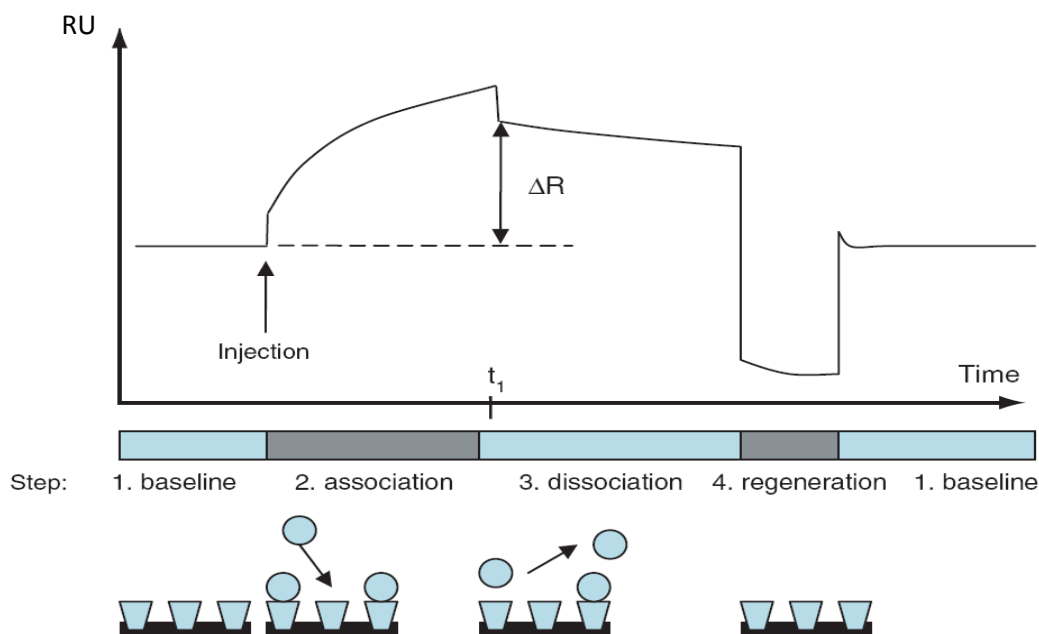


Figure 2.2.4: Sensorgram showing the steps of an analysis cycle: 1. the buffer is in contact with the sensor (baseline); 2. continuous injection of sample solution (association); 3. buffer injection (dissociation step); ΔR indicates the measured response due to the bound target compound; 4. removal of bound species from the surface during injection of regeneration solution (regeneration step) followed by a new analysis cycle. A bulk refractive index shift can be observed at t_1 .

Each measurement starts with conditioning the sensor surface with a suitable buffer solution (1). It is of vital relevance to have a reliable baseline before the capturing event starts. At this point, the sensor surface contains the active ligands, ready to capture the target analytes. On injecting the solution containing the analytes (2), they are captured on the surface. Also other components of the sample might adhere to the sensor surface; without a suitable selection of the ligand, this adherence will be non-specific, and thus easy to break. At this step, adsorption kinetics of the analyte molecule can be determined in a real-time measurement. Next, buffer is injected on to the sensor and the non-specifically bound components are flushed off (3). As indicated in the figure, the accumulated mass can be obtained from the SPR response (ΔR). Also in this step, dissociation of the analyte starts, enabling the kinetics of the dissociation process to be studied. Finally, a regeneration solution is injected, which breaks the specific binding between analyte and ligand (4). If properly anchored to the sensor surface, the ligands remain on the sensor, whereas the target analytes are quantitatively removed. Again, buffer is injected to condition the surface for the next analysis cycle.

Often SPR measurements are carried out to determine the kinetics of a binding process. Pseudo first-order kinetics are assumed, and the change in SPR angle is recorded as a function of time. Reaction rate constants of interactions can be determined, e.g. the interaction $A+B=AB$ can be followed in real time where A is the analyte and B is the ligand immobilized on the sensor surface. Table 2.2 contains the most relevant kinetic parameters, the association and dissociation constants, for the simplest case $A+B=AB$.

Table 2.2: Definitions of the most relevant kinetic parameters: association and dissociation constants.

	<i>Association rate constant, k_a</i>	<i>Dissociation rate constant, k_d</i>
Definition	$A + B \rightarrow AB$	$AB \rightarrow A + B$
Description	Reaction rate of AB formation: number of AB complexes formed per unit time at unit concentration of A and B	Dissociation rate of AB: number of AB complexes dissociating per unit time
Units	$\text{l mol}^{-1} \text{s}^{-1}$	s^{-1}
Typical range	$10^3 - 10^7$	$10^{-1} - 5 \times 10^{-6}$

The association constant is the reaction rate of complex (AB) formation, giving the number of complexes formed per time at unit concentration of A and B. As soon as the complex AB is formed, its dissociation can start. The dissociation rate constant describing this process expresses the number of AB complexes dissociating per unit time. Association rate constants can be measured ranging from 10^3 to $10^8 \text{ M}^{-1} \text{ sec}^{-1}$ and dissociation rate constants from 10^{-5} to 1 sec^{-1} [147].

BIAevaluation software's equipped with different kinetic models allow the calculation of affinity constants ($K_D = k_{\text{association}}/k_{\text{dissociation}}$) from experimentally obtained association and dissociation rate constants. The typical working range for affinity measurements with Biacore's biosensors is picomolar to high micromolar for K_D (M).

The biosensors used in this thesis were Biacore 2000 and Biacore S51.

Biacore 2000 is currently the most widely used Biacore instrument. It is equipped with a robotic autosampler and can be programmed through the use of wizards or methods in the control software to automatically inject samples for up to two 96-well microtiter plates. The fluidic system in this instrument creates four serially linked flow cell areas on one sensor chip, thereby increasing the potential number of simultaneous measurements. For example, it is possible to simultaneously collect data from a reference surface as well as three other surfaces with different immobilized ligands as well as reference-subtracted data for each surface.

Biacore S51, instead, offers a unique platform designed for screening applications and kinetic characterization of low-molecular weight compound leads. There are two independent flow cells in Biacore S51, each of which contains three detection spots. The central spot is used as a reference surface, while different molecules can be immobilized on the outer two spots using hydrodynamic addressing.

3. MATERIALS AND METHODS

3.1 CELL CULTURE AND TREATMENTS

To study the effects of the administration of FR18 on colon carcinoma cells we used the HT-29 cell line (Zooprofilatic Institute of Brescia, Italy). The human epidermoid cell line, A431 (Zooprofilatic Institute of Brescia, Italy) was also used to perform surface plasmon resonance (SPR) studies.

Both cell lines were propagated in monolayer cultures in RPMI 1640 (Euroclone, Milan, Italy) medium inoculated at a density of 10^4 cells/cm². The medium was supplemented with 10% (v/v) heat-inactivated (56°C for 20 min) fetal bovine serum (FBS) (Euroclone, Milan, Italy) and with 2 mM L-glutamine (Sigma-Aldrich, St. Louis, MO). Cells were kept in an incubator at 37°C in 5% CO₂ atmosphere and splitted every five-six days. Before splitting the cells were washed twice with phosphate buffer PBS, consisting of 8 g/L NaCl (Sigma-Aldrich, St. Louis, MO), 1.15 g/L Na₂PO₄ (Sigma-Aldrich, St. Louis, MO), 0.20 g/L KH₂PO₄ (Sigma-Aldrich, St. Louis, MO), 0.20 g/L KCl (Sigma-Aldrich, St. Louis, MO), then detached with 0.11% Trypsin (Sigma-Aldrich, St. Louis, MO)/0.02% ethylenediaminetetraacetic acid (EDTA) (Sigma-Aldrich, St. Louis, MO) for 5 min at 37°C. Detached cells were subsequently resuspended in fresh medium and counted in a Burker chamber.

FR18, 2-(8-amino-octylamino)-[1,4]naphthoquinone, synthesized in the laboratory of Professor Melchiorre (Department of Pharmaceutical Sciences, University of Bologna, Italy), was dissolved in dimethyl sulfoxide (DMSO) (Sigma-Aldrich, St. Louis, MO) at a concentration of 10 mM and stored at +4°C as a stock solution. The drug was diluted in fresh medium before each experiment. EGF was purchased from Oncogene (Cambridge, MA), dissolved in 10 mM acetic acid at 100 µg/ml, and stored at -20°C. Alexa Fluor[®] 488 EGF complex (Invitrogen, Carlsbad, CA), was dissolved in 200 µg/mL stock solutions in phosphate-buffered solution, containing 1% BSA with the addition of sodium azide at a final concentration of 2 mM, and stored at -20°C. EGF and fluorescent EGF were diluted in RPMI 1640 before each experiment at the indicated concentrations. Cells were serum starved according to experimental needs that is, cultured in RPMI 1640 medium supplemented with 0.25% FBS (v/v).

3.2 CELL PROLIFERATION ASSAY

The cell growth inhibitory effect of FR18 on HT-29 cells was determined by using the 3-(4,5-dimethylthiazol-2-yl)-2,5-diphenyltetrazolium bromide (MTT) (Sigma-Aldrich, St. Louis, MO) assay [148].

This assay is based on a colorimetric reaction, catalyzed by the mitochondrial succinic dehydrogenase enzyme, which converts the substrate (MTT) in a water insoluble formazan salt. The formation of this salt is a sign of cell integrity and therefore viability. HT-29 cells inoculated in 96 multiwell plates at a density of 10^4 cells/cm² after 24 hours of adhesion were treated in triplicate with increasing concentrations of FR18 in the range 10 nM-1.2 mM, for 24 hours.

After treatment, cells were deprived of culture medium, spiked with 200 μ L of a solution of MTT (0.2 mg/ml) in PBS and incubated for 2 hours at 37 ° C. The MTT solution was removed and the formazan salts solubilised in 200 μ L of isopropanol (Sigma-Aldrich, St. Louis, MO) for 20 min in agitation at room temperature. The absorbance of the coloured solution was quantified at 570 nm using the Victor2 Wallac 1420 multilabel counter spectrophotometer.

The IC₅₀ value was calculated according to the GraphPad Prism 3.02 software relating the optical density at 570 nm with the logarithm of molar concentrations of FR18.

3.3 CONFOCAL LASER SCANNING MICROSCOPY

For confocal microscopy HT-29 were inoculated at a density of 10^4 cells/cm² in 6 multiwell plates on borosilicate glass coverslips of 0.13 mm average thickness.

After 24 hours of adhesion cells were serum starved for 48 hours and then treated for 30 min with 5 μ g of Alexa Fluor[®] 488 EGF complex (Invitrogen, Carlsbad, CA), or both 2 μ M FR18 and 5 μ g of Alexa Fluor[®] 488 EGF complex. The reagents were both dissolved in serum-free fresh medium. For spectral imaging, preparations were washed with RPMI 1640, fixed with 3% paraformaldehyde, and embedded in mowiol (Hoechst, Frankfurt, Germany). Alexa Fluor[®] 488 was excited at 488 nm with an argon laser, and fluorescence was detected in spectral mode (Nikon C1s confocal laser-scanning microscope) in the interval 500-550 nm at 5 nm resolution.

At least five cells were measured and the signal was corrected for background fluorescence by subtracting the average of the fluorescence detected from at least five extracellular regions from the same spectral image.

For EGF/EGFR complex confocal analysis, cells were treated with FR18 and Alexa Fluor[®] 488 EGF complex, as described. The preparations were then washed twice in PBS, fixed with 3% paraformaldehyde (Sigma-Aldrich, St. Louis, MO) for 10 min at room temperature, washed thrice in 0,1 M glycine (Sigma-Aldrich, St. Louis, MO) in PBS and permeabilized with 70% ice-cold ethanol for 2-3 min at -20°C.

For indirect immunofluorescence, cells were left in agitation with 1% BSA in PBS for 60 min at room temperature and then incubated overnight at 4°C with the monoclonal primary antibody against EGFR (Biosource, Camarillo, CA) at a final concentration of 0.2 µg/mL in BSA/PBS. Subsequently the samples were washed twice with BSA/PBS and incubated for 1 h at room temperature with Alexa 568-conjugated secondary antibody 1:1,000 in BSA/PBS.

Multiple images were acquired by using sequential laser excitations at 488 and 568 nm to reduce spectral bleedthrough artifacts. The images were collected by using a BioRad MRC1024 UV confocal microscope, equipped with a Nikon PlanApo 60X, 1.4-NA oil immersion lens, and analyzed by Image J (W.S. Rasband, ImageJ, NIH, Bethesda, MD, USA, <http://rsb.info.nih.gov/ij/>, 1997–2006).

3.4 FLOW CYTOMETRY ANALYSIS

Cells were treated for 24 h with FR18 (1 nM-5 µM) or 3 µg/mL anti-EGFR monoclonal antibody (Chemicon, Temecula, CA), detached by trypsinization, washed in PBS, and centrifuged at 240 g for 10 min. The pellet was resuspended in 0.01% Nonidet P-40 (Sigma-Aldrich, St. Louis, MO), 10 µg/mL RNase (Sigma-Aldrich, St. Louis, MO), 0.1% sodium citrate, 50 µg/mL propidium iodide (PI) (Sigma-Aldrich, St. Louis, MO) for 30 min at room temperature in the dark. The relationship between the quantity of cells to be analyzed and the volume of the solution was 10⁶ cells/mL.

Propidium iodide is a fluorescent probe that binds stoichiometrically to DNA by intercalating between the bases with little or no sequence preference, it is excited at 495 nm and emits at 639 nm. The intensity of fluorescence emitted is proportional to the amount of DNA present in each cell.

PI fluorescence was analyzed by using a flow cytometer Epics XL MCL (Coulter), and cell cycle analysis was performed using the MCycle (Verity) and MODFIT 5.0 softwares. All experiments were repeated at least twice.

3.5 EGFR PHOSPHORILATION STATE ANALYSIS

3.5.1 Treatments

After 24 h of adhesion, HT-29 were serum starved for two days before being exposed to 2 μ M FR18, dissolved in serum-free fresh medium, for 30 min. Cells were washed in RPMI 1640, treated for 30 min with 100 pM EGF and lysed directly in the culture plate.

3.5.2 Protein extraction: whole cell lysate

Adherent cells were washed twice with 1 mL of cold PBS-1mM vanadate and lysed in 500 μ L of RIPA buffer [10 mM Tris-HCl (Sigma-Aldrich, St. Louis, MO), pH 7.5, 150 mM NaCl, 1 mM NaF (Fluka), 1% EDTA modified with 1% Na-deoxycholate (Sigma-Aldrich, St. Louis, MO), 0.1% sodium dodecyl sulfate (SDS) (ICN Biomedicals, Irvine, CA), protease inhibitors (0.01 mg/mL aprotinin, 0.01 mg/mL antipain, 0.01 mg/mL leupeptin, 0.01 mg/mL pestatin) (Inalco, Milan, Italy), 0.1 mM phenylmethyl sulfonyl fluoride (PMSF), 0.5 mM sodium vanadate (Sigma-Aldrich, St. Louis, MO)] and 500 μ L of HNTG buffer [50mM HEPES (Sigma-Aldrich, St. Louis, MO) pH 7.4, 150mM NaCl, 0.1% Triton X-100 (Sigma-Aldrich, St. Louis, MO), 10% glycerol].

After 15 min at 4°C, the lysates were spun at 14,000 rpm at 4°C for 20 min. The supernatants were used as whole cell extracts.

3.5.3 Determination of protein concentration

Protein concentration was determined by using the Bradford protein determination method. First a calibration curve with known concentrations of BSA was prepared. Protein samples (BSA or cell lysates) were added with the Bradford reagent (Coomassie Brilliant Blue G-250) (Bio-Rad, Richmond, CA) and their absorbance at 595 nm was measured using an Uvikon 930 (Kontron) spectrophotometer. Protein concentration for each cell lysate was determined by interpolation of the absorbance on the calibration curve obtained from the samples at known protein concentration.

3.5.4 Immunoprecipitation and Western Blot

Five hundred micrograms of proteins were immunoprecipitated overnight at 4°C with 1 µg of anti-EGFR monoclonal antibody (Biosource, Camarillo, CA) in 700 µL of lysis buffer.

Protein A Sepharose CL-4B (Amersham, Pittsburg, PA) was activated by adding 1 mL of HCl (Carlo Erba, Milan, Italy) 1mM. The resin was left on ice for 20 min and washed thrice in 1 mM HCl and 0.1 M NaHCO₃ buffer (Sigma-Aldrich, St. Louis, MO) in 0.5 M NaCl at pH 8, centrifuging each time for 3 min 3,000 g. The resin was finally resuspended at a concentration of 6 mg/30 µL of bicarbonate buffer at pH 8.

Previously obtained immune complexes were added to 6 mg of resin, kept in a shaker for 45 min at room temperature and precipitated at 13,000 g for 30 min. The obtained pellets were washed from any excess of extracted protein with 0.1 M potassium phosphate buffer (KH₂PO₄ / K₂HPO₄) at pH 8, centrifuging each time for 5 min at 10,000 g and subsequently resuspended in 20 µL of Sample buffer (65 mM Tris-HCl at pH 7.5, 65 mM β-mercaptoethanol, 1% SDS, 10% glycerol, 0.001% bromophenol blue). Samples were heated for 5 minutes at 100 °C, cooled on ice, centrifuged for 30 sec at maximum speed and the supernatants were electrophoresed for 60 min on 7.5% (w/v) polyacrylamide gels using 200 V constant voltage at +4°C.

The running buffer was 0.025 M Trizma base (Sigma-Aldrich, St. Louis, MO), 0.192 M Glycine (Sigma-Aldrich, St. Louis, MO), 10% SDS (Sigma-Aldrich, St. Louis, MO) in H₂O.

The gel was maintained for 20 min in agitation in the transfer buffer consisting of 0.025 M Trizma base, 0.192 M Glycine, 10% methanol in double-distilled H₂O.

Simultaneously, the nitrocellulose membrane (Schleicher & Schuell BioScience, Keene, NH), was activated by a first wash of 5 min in double distilled H₂O, and a second one in transfer buffer for 20 min.

Proteins were electrophoretically transferred to the nitrocellulose transfer membrane for 60 min using 100 V constant voltage at room temperature.

The membrane was blocked in 0.1% PBS-Tween 20 (Sigma-Aldrich, St. Louis, MO) for 60 min at room temperature and incubated overnight at +4°C or 1 h at room temperature with anti-phosphotyrosine monoclonal antibody (Upstate Biotechnology, Lake Placid, NY) diluted 1:1,000 in 0.1% PBS-Tween 20. The membrane was washed in 0.1% PBS-Tween 20 (two times for a few seconds, once for 15 min, twice for 5 min), incubated for one hour, with a solution containing the appropriate horseradish peroxidase-linked secondary antibody (Amersham, Pittsburg, PA) diluted 1:20,000 in 0.1% PBS-Tween 20 and washed again with PBS-Tween 20.

Immunoreactive bands were finally developed with SuperSignal West Dura Extended Duration chemiluminescent substrate according to the manufacturer's protocol (Pierce, Rockford, IL).

3.6 EGF/EGFR COMPLEX INTERACTION STUDIES BY SURFACE PLASMON RESONANCE

To study the EGF/EGFR complex interaction three different experimental approaches have been used.

EGFR immobilisation, directly or via capturing antibodies, on a sensor chip and its interactions with EGF were studied. An EGFR over expressing human epidermoid carcinoma cell line, A431 (2×10^6 EGFR molecules/cell) was used as receptor source [149, 150]. Also EGF was immobilised and its interaction with the receptor from A431 cell lysate was investigated.

A commercially available purified EGF receptor (Sigma-Aldrich, St. Louis, MO) was subsequently immobilised on a sensor chip and its interaction with EGF was assayed.

3.6.1 EGFR capturing from A431 total cell lysate and binding to EGF

For EGF/EGFR interaction study, EGFR immobilisation from A431 cell lysate via two capturing antibodies that recognise its C-terminal region and a lipid bilayer environment reconstitution on the chip surface were investigated.

Solubilization of EGFR receptors

Approximately 10^7 cells were lysed in 1mL of RIPA modified buffer as described in chapter 3.5.2 or in a buffer consisting of PBS, pH 7.4, 0.01 mg/mL of each protease inhibitor (aprotinin, antipain, leupeptin, pepstatin), 0.1 mM phenylmethyl sulfonyl fluoride (PMSF), 0.5 mM sodium vanadate and 1% Triton X-100 on a rocker for 45min at 4°C. Cell lysates were clarified using a tabletop centrifuge at 14,000 rpm for 30 min at 4°C and the supernatants containing the EGFR receptors were transferred to new tubes.

Preparation of lipid/detergent-mixed micelle

To prepare lipid/detergent-mixed micelles, aliquots of 2.5 mg of a lipid mixture containing 16.7% phosphatidylethanolamine, 10.6% phosphatidylserine, 9.6% phosphatidylcholine, 2.6% phosphatidic acid, 1.6% phosphatidyl inositol, 58.7% other lipids (Avanti Polar Lipids Inc., Alabaster, AL) were transferred into glass test tubes. A thin lipid film was formed on the glass wall by rotating the tube while evaporating the chloroform using a stream of nitrogen gas. Any

remaining chloroform was removed using overnight vacuum. To these dry lipid aliquots, 1ml of HBS buffer [10 mM HEPES (Sigma-Aldrich, St. Louis, MO), pH 7.4, and 0.15 M NaCl] supplemented with 30 mM n-Octyl- β -D-glucoside detergent (Anatrace, Maumee, OH) was added and the mixtures were vortex three times.

EGFR capturing and interaction with EGF

EGFR antibodies (abcam plc, Cambridge, UK and Santa Cruz Biotechnology, Santa Cruz, CA) were buffer changed in 10 mM sodium acetate at pH 5.0 and pH 4.5 respectively using the protein desalting spin columns (Pierce, Rockford, IL) according to manufacturer's instruction and 25 μ g/mL of each antibody was immobilized on the chip by amine coupling.

The sensor chip surface was activated by a 7 min injection of 0.1 M N-hydroxysuccinimide (NHS) (GE Healthcare, Uppsala, Sweden) mixed 50:50 with 0.4 M N-ethyl-N'-dimethylaminopropylcarbodiimide (EDC) (GE Healthcare, Uppsala, Sweden). Antibodies were injected on the surface for 7 minutes at 5 μ L/min flow rate and the surface was subsequently deactivated by a 7 min injection of 1 M ethanolamine pH 8.5 (GE Healthcare, Uppsala, Sweden).

Total cell lysate containing the EGFR was injected for 20 min at 5 μ L/min flow rate across the antibodies immobilised surfaces on separate flow cells of the L1 chip employing the COINJECT function. In sequence with the receptor capture a lipid bilayer was reconstituted by injecting the lipid mixture for 10 min at 5 μ L/min flow rate [151]. A reference surface (negative control) where solubilized receptor was not injected across the antibodies immobilised surface, followed by reconstitution was also included.

Increasing concentrations 20 nM-1 μ M of EGF (PreproTech, Rocky Hill, NJ) and HBS buffer (blank) were injected over the activated surfaces for 3 min at a flow rate of 30 μ L/min in order to study EGF/EGFR interaction. EGF was allowed to dissociate for 10 min in absence of surface regeneration.

All experiments were performed using a Biacore 2000 instrument (GE Healthcare, Uppsala, Sweden) equipped with an L1 sensor chip (GE Healthcare, Uppsala, Sweden) which consists of a thin gold-film covered with a carboxymethylated dextran-matrix modified with lipophilic substances (www.biacore.com) and the running buffer was HBS buffer.

3.6.2 EGF immobilization and binding to EGFR

EGF was also immobilised on the sensor chip in order to investigate its interaction with EGFR present in two different cell lysates.

Solubilization of EGFR receptors

10^7 A431 cells were lysed in 1mL of PBS containing 10mM EDTA, 1mM PMSF, 0.1 mg/mL aprotinin and 1% TritonX-100 (bufferA) for 30 min on ice [152] or in 1 mL of 50mM Tris-HCl, pH 7.4, 50 mM MgCl₂, 10 μM sodium vanadate, 5 mg/mL aprotinin, 1 mM EDTA and 1mM PMSF (buffer B) for 20 min at +4°C and clarified by centrifugation at 10,000 rpm for 15 min at +4°C [153] and the supernatants containing the EGFR receptors were transferred to new tubes.

EGF was buffer changed in 10 mM sodium acetate, pH 4.5 using the protein desalting spin columns (Pierce, Rockford, IL) and a 100 μg/mL solution was amine coupled on an L1 sensor chip for 10 min at 5 μL/min of flow rate using a Biacore S51 instrument (GE Healthcare, Uppsala, Sweden) and HBS as running buffer. A reference surface (negative control) was activated and deactivated in the same way as the respective active surface.

Total cell lysate containing the EGFR was injected for 20 min at 10 μL/min flow rate across the EGF immobilised surfaces. Subsequently a lipid bilayer was reconstituted by injecting the lipid mixture for 10 min at 10 μL/min flow rate (as described in chapter 3.6.1).

3.6.3 Purified EGFR immobilization and binding to EGF

Commercial EGFR isolated from A431 cells by affinity-purification (Sigma-Aldrich, St. Louis, MO) was reconstituted in 10% glycerol in sterile water, yielding a 278 μg/mL stock solution in 50 mM HEPES, pH 7.6, 150 mM NaCl, 0.05% Triton X-100, 10% glycerol, 1 mM dithiothreitol and 10% trehalose.

EGFR-stock diluted to 56 nM with 9 mM sodium acetate buffer, pH 5.0, 10% glycerol, 1 mM DTT and 0.05% TritonX-100 was immobilized on the chip by amine coupling as previously described. EGFR was injected on the sensor chip for 12 minutes at 5 μL/min flow rate. A reference surface was activated and deactivated in the same way as the respective active surface.

To study the EGF/EGFR interaction, four consecutive running buffer (20 mM Tris-HCl, pH 7.4, 150 mM NaCl, 1 mM EDTA, 0.05% TritonX-100, 1 mM DTT and 10% glycerol) cycles were run

on the sensor chip surface followed by triplicate injections of EGF for 7 min at 5 $\mu\text{L}/\text{min}$ in order of increasing concentration (15 nM-2 μM). EGF was allowed to dissociate for 5 min before regenerating the chip surface for 1 min with 10 mM glycine, pH 2.0. Biacore S51 instrument equipped with L1 sensor chip was used.

4. RESULTS

4.1 CELL VIABILITY ASSESMENT

To assess the cytotoxic effects of FR18 in our experimental model (HT-29), the dose inhibiting the growth of 50% of the cell population (IC_{50}) was initially determined by MTT assay as described in section 3.2.

After 24 h of adhesion, HT-29 cells were exposed to increasing concentrations of FR18 (10 nM-1.2 mM) and absorbance values obtained at 570 nm as a function of the logarithm of molar concentration of FR18 were reported in the chart below. As shown in Figure 4.1, HT-29 cells were sensitive to FR18 with an approximate IC_{50} of 45.16-58.80 μ M.

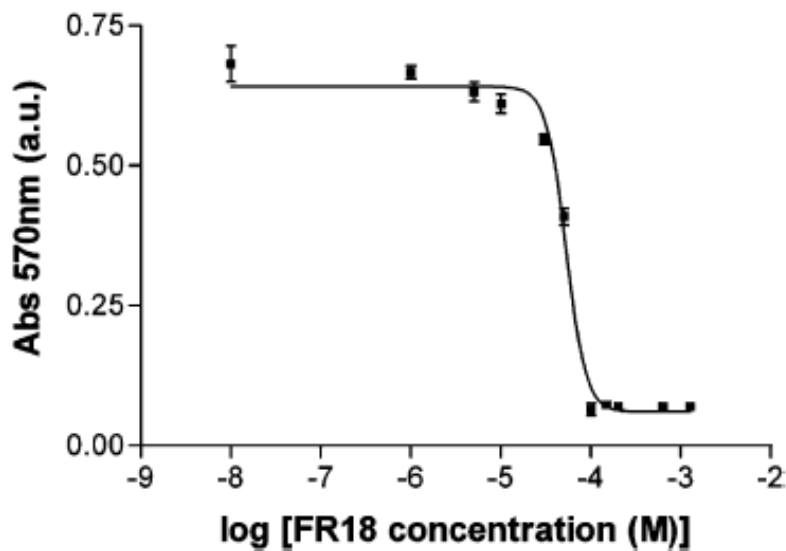


Figure 4.1: Inhibitory effects of FR18 on HT-29 cells proliferation. Cells were incubated with increasing concentrations of FR18 for 24 h. The cell viability was determined by MTT assay. Data are shown as means \pm SD (n = 3).

4.2 FR18 EFFECTS ON EGF/EGFR INTERACTION

Fluorescence confocal microscopy was used to investigate specific binding of FR18 to EGFR. Due to the structural similarity to shikonin, it was assumed that FR18 would interfere with the binding mechanisms of EGF to its receptor. The experiments were therefore performed with a fluorescent EGF derivative (Alexa Fluor[®] 488 EGF) and the confocal microscopy analysis revealed that EGF and EGFR formed a complex localized in granules in the plasma membrane in EGF-stimulated serum-starved cells, whose presence greatly diminished in FR18-treated and EGF-stimulated HT-29. This indicated that concomitant treatment with FR18 and EGF prevented the complex formation (Figure 4.2.1). In addition, spectral imaging was applied to confirm and quantify the interference of FR18 on EGF/EGFR interaction. As shown in Figure 4.2.2, EGF-associated fluorescence signal decreased threefold in the presence of FR18.

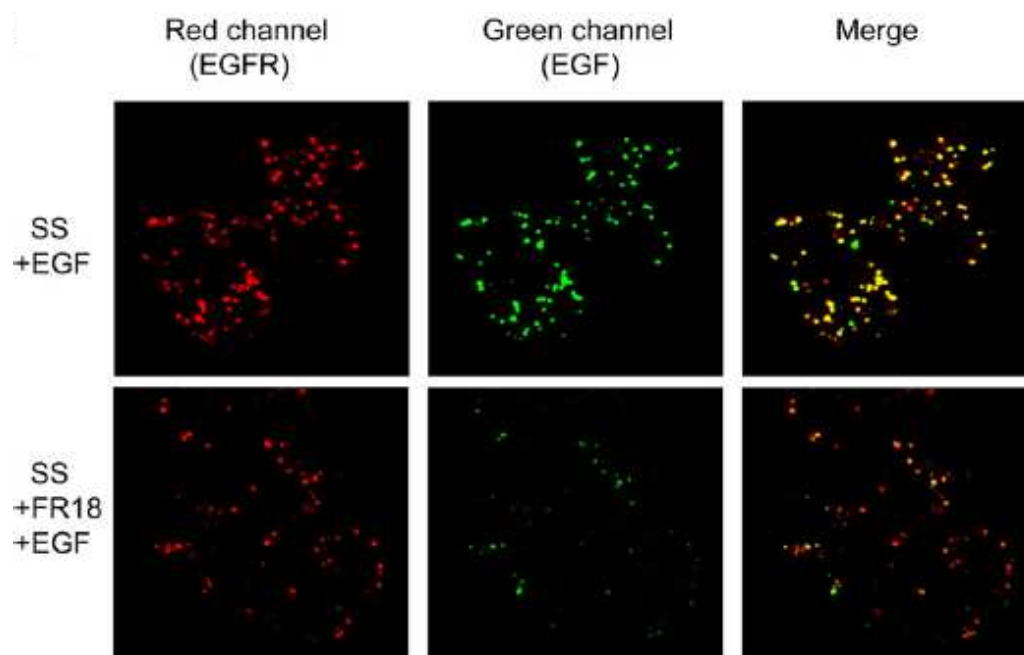


Figure 4.2.1: Confocal laser-scanning micrographs and confocal spectral analysis of EGF and EGFR in control and FR18 treated cells. Staining of EGF (green fluorescence) and EGFR (red fluorescence) in control and in FR18 treated cells are shown in upper panels and in lower panels, respectively. Manders' overlap coefficient of EGF signal coincident with EGFR signal is 0.43 in treated cells and 0.79 in untreated HT-29. The images were collected using a Nikon Plan Apo 60 \times , 1.4-NA oil immersion lens.

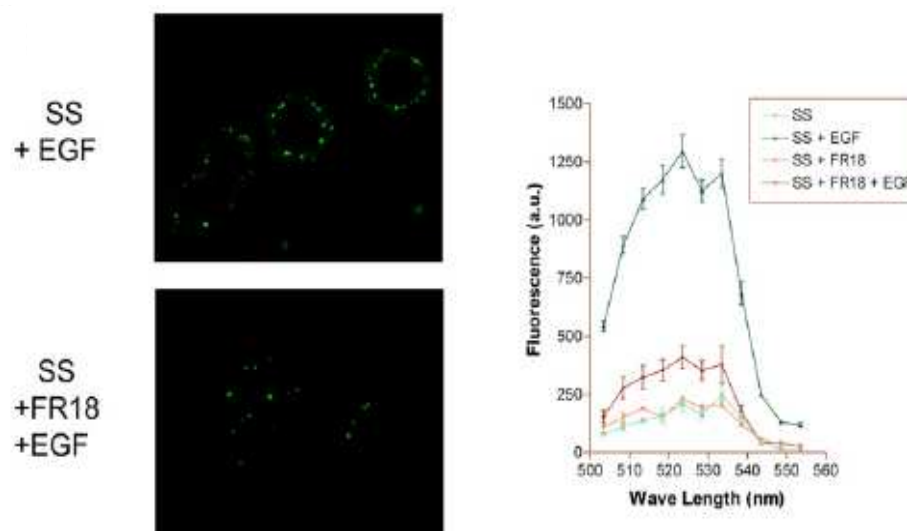


Figure 4.2.2: Spectral confocal imaging of EGF binding to EGFR. Left) Representative spectral micrographs, right) collected spectra from at least five cells for each acquisition.

4.3 CELL CYCLE ANALYSIS AND APOPTOSIS EVALUATION

To determine the effects of FR18 on the growth of HT-29, cells were treated for 24 hours with FR18 (1 nM-5 μ M) or with an anti-EGFR monoclonal antibody that blocks the ligand binding site. Cells were permeabilized, incubated with RNase and labeled with propidium iodide, as described in section 3.4.

The fluorescence associated with propidium iodide was analyzed using a flow cytometer Epics Elite (Coulter) equipped with an Argon ion laser.

The cell cycle was analyzed using the software M Cycle (Verity) and MODFIT 5.0.

FR18 treatment resulted in a dose-independent arrest in the S phase. In addition, an apoptotic peak was detected for higher concentrations (30 nM-5 μ M). Peak average was 8.06% for 30 nM FR18 treatment and increased to 26.06% for 5 μ M (Figure 4.3).

On the contrary, treatment of HT-29 cells with an anti-EGFR mAb that blocks the ligand binding site determined a cell cycle arrest in G0/G1 and did not induce apoptosis (Figure 4.3).

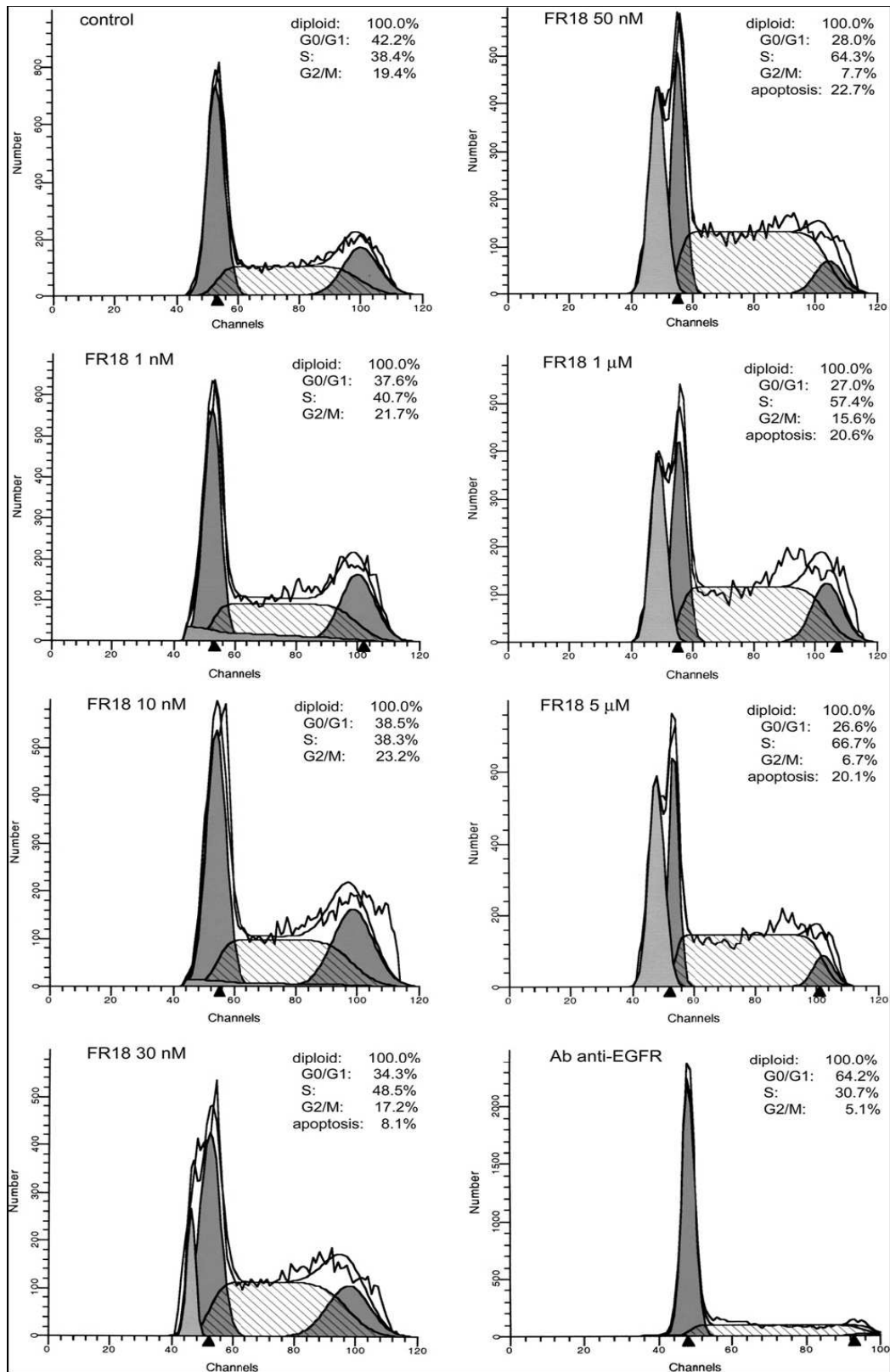


Figure 4.3: Flow cytometric analysis of HT-29 cells treated with FR18 or an anti-EGFR monoclonal antibody for 24 h. Cell cycle in phase S arrest and apoptosis were observed at concentrations ranging from 1 nM to 5 μM. In anti-EGFR monoclonal antibody treated samples instead, a proliferation arrest in G0/G1 was detected.

4.4 FR18 EFFECTS ON EGFR PHOSPHORILATION

As binding of EGF caused EGFR activation through dimerization and phosphorylation of tyrosine residues in its cytoplasmic domain immunoblot experiments with anti-phosphotyrosine antibody was performed. Treatment with EGF for 30 min of serum-starved HT-29 resulted in EGFR activation, and a comparable receptor phosphorylation pattern was recorded after exposure to EGF in combination with FR18 as shown in Figure 4.4.

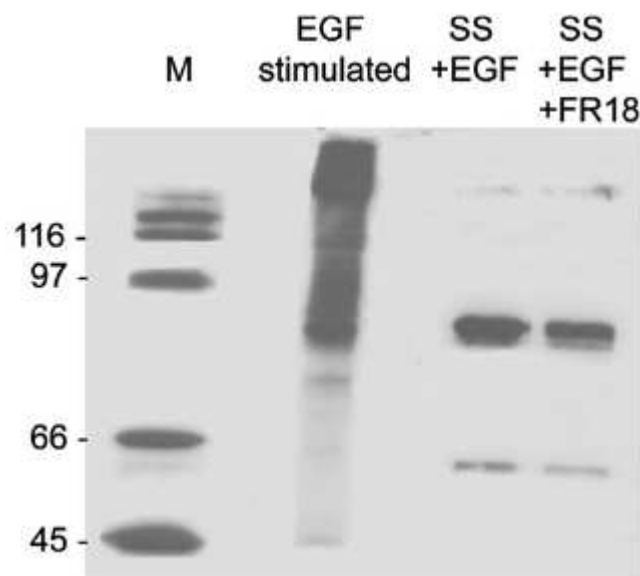


Figure 4.4: Effect of FR18 on EGFR phosphorylation. Serum-starved HT-29 cells were treated with 2 μ M FR18 for 30 min and then incubated with 100 pM EGF for 30 min. Cell lysates were immunoprecipitated with an anti-EGFR antibody and immunoblotted with an anti-phosphotyrosine antibody. Detection of immunoreactive bands was performed with secondary antibody conjugated with horseradish peroxidase and developed with a chemiluminescent system.

4.5 SPR STUDIES OF EGF/EGFR INTERACTION

4.5.1 EGF binding to captured and reconstituted EGFR from A431 cell lysate

For EGF receptor capturing on the L1 surface A431 cell lysate was used as receptor source. To form more active and oriented anti-EGFR antibody surfaces, amine coupling chemistry was used to immobilize both antibodies purchased from Abcam Plc (Cambridge, UK) and Santa Cruz Biotechnology (Santa Cruz, CA) at similar densities on the L1 chip surface resulting in a range of 10-13 kRU.

Across these antibody prepared surfaces A431 cell lysate was injected for 20 min, followed by an immediate reconstitution of lipids with a 10 min injection of 2.5 mM lipid mixture and 30 mM n-Octyl-b-D-glucoside detergent using the COINJECT function, resulting in both cases where cell lysate in RIPA and PBS buffer were used as receptor source, in 600-750 RU of density.

To verify the presence of captured and reconstituted EGF receptor, increasing concentrations of EGF (20 nM-1 μ M) and HBS buffer (blank) injections were run through the active and reference surfaces for 3 min at 30 μ L/min of flow rate and the dissociation was followed for 10 min in absence of surface regeneration.

As shown in figure 4.5.1-1 no binding to the active or to the reference surface was observed indicating that very low quantities or inactive EGFR capture had occurred when cell lysate in PBS buffer was used as EGFR source.

EGF binding to the active surfaces, obtained using cell lysate in RIPA buffer and anti-EGFR from Santa Cruz Biotechnology (Santa Cruz, CA) for EGFR capturing and reconstitution, was observed instead at very low levels. A maximum response of 5 RU was recorded and only for EGF concentrations ranging from 20-160 nM (Figure 4.5.1-2), indicating that the quantity of active EGFR captured and reconstituted on the chip surface was extremely low. All experiments were performed using a Biacore 2000 instrument and shown sensograms were reference and blank subtracted.

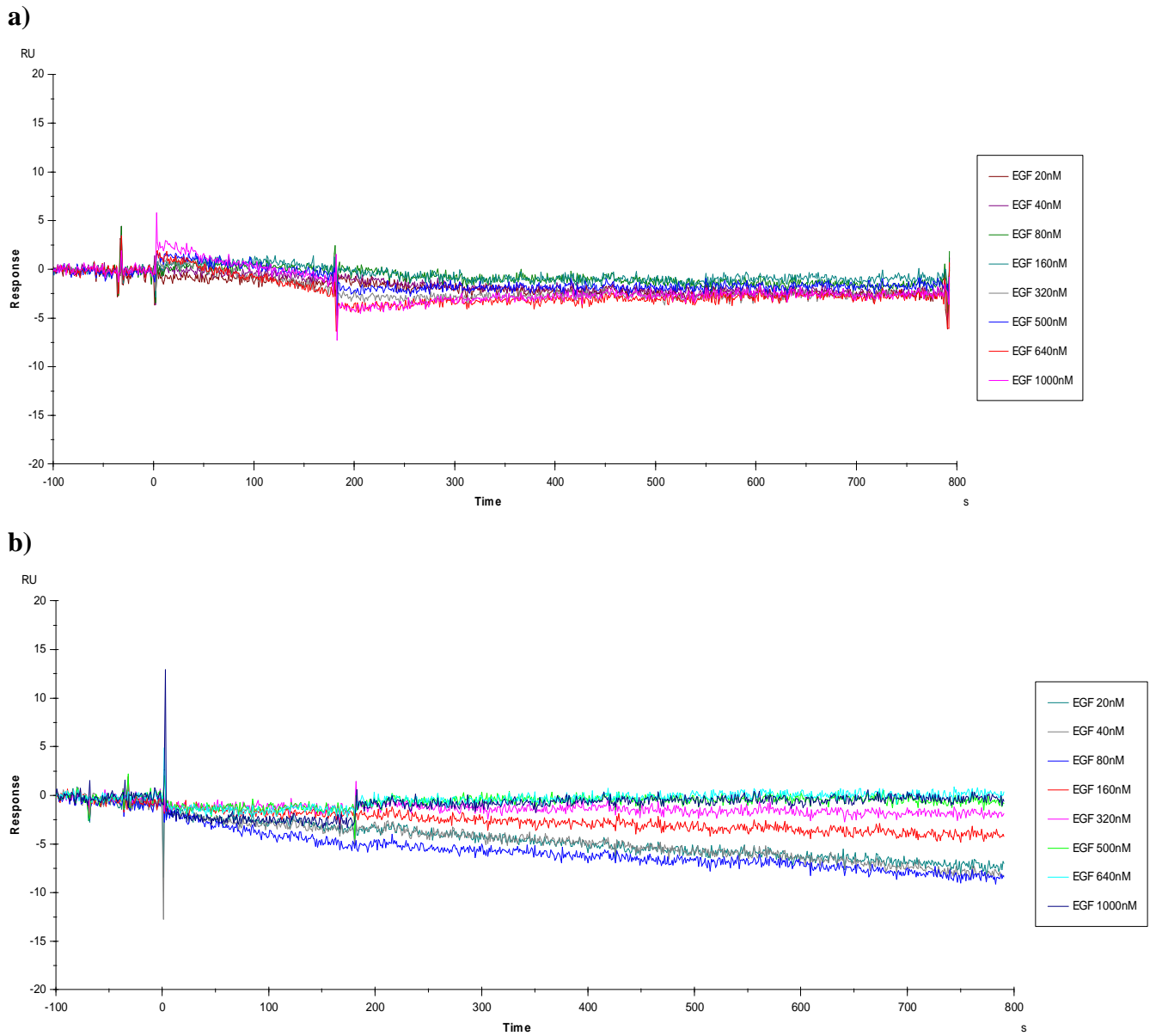


Figure 4.5.1-1: EGF binding to active surfaces obtained using cell lysate in PBS buffer as EGFR source and anti-EGFR purchased from **a)** abcam plc (Cambridge, UK) and **b)** Santa Cruz Biotechnology (Santa Cruz, CA) for receptor capturing.

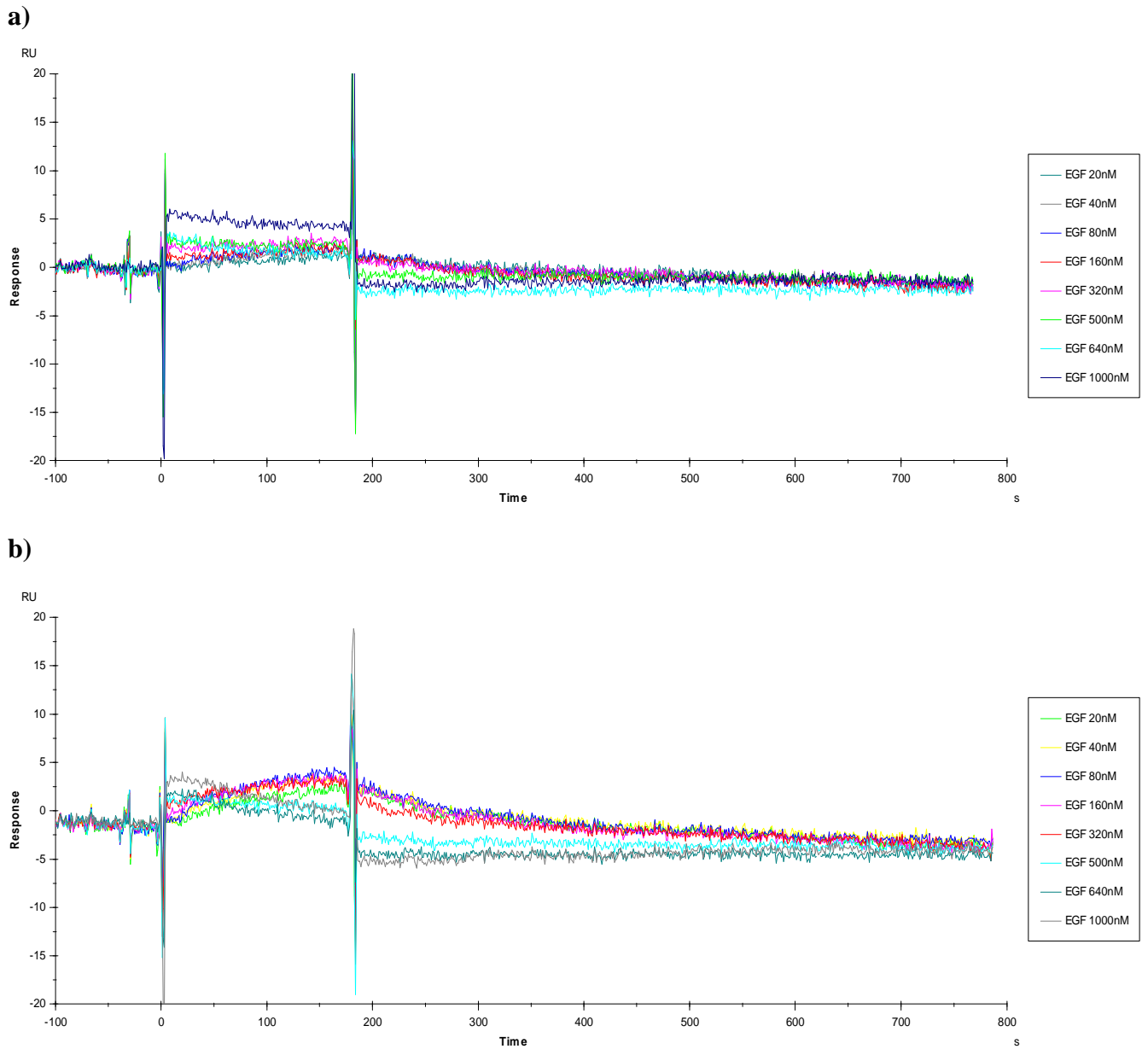


Figure 4.5.1-2: EGF binding to active surfaces obtained using cell lysate in RIPA buffer as EGFR source and anti-EGFR purchased from **a)** abcam plc (Cambridge, UK) and **b)** Santa Cruz Biotechnology (Santa Cruz, CA) for receptor capturing and reconstitution. Only 5 RU of not concentration-dependent binding response was observed when anti-EGFR antibody from Santa Cruz Biotechnology (Santa Cruz, CA) was used.

4.5.2 Immobilised EGF interaction with A431 cell lysate

For EGF/EGFR complex interaction studies, EGF was also used for EGFR capturing on L1 sensor chip. EGF was immobilised on the sensor chip by amine coupling chemistry and its interaction with two different A431 total cell lysate (EGFR source) was examined. Biacore S51 instrument was used for all experiments.

EGF was buffer changed in 10 mM sodium acetate buffer, pH 4.5 and a solution of 100 µg/mL was injected on the chip surface for 10 min at 5 µL/min of flow rate resulting in 800 RU of immobilisation response as shown in figure 4.5.2-1.

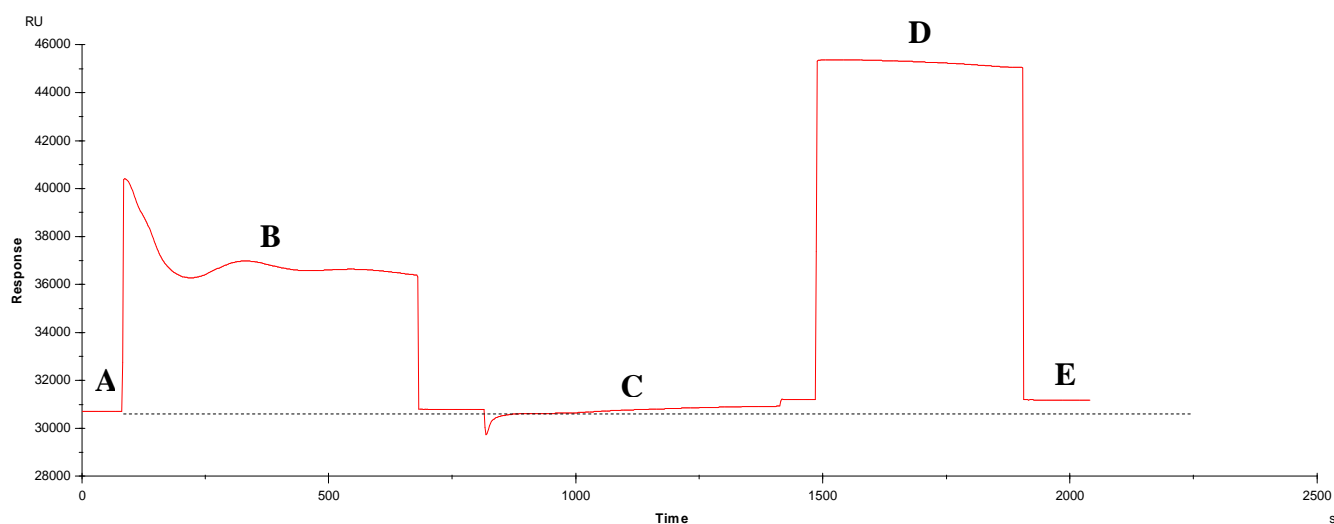
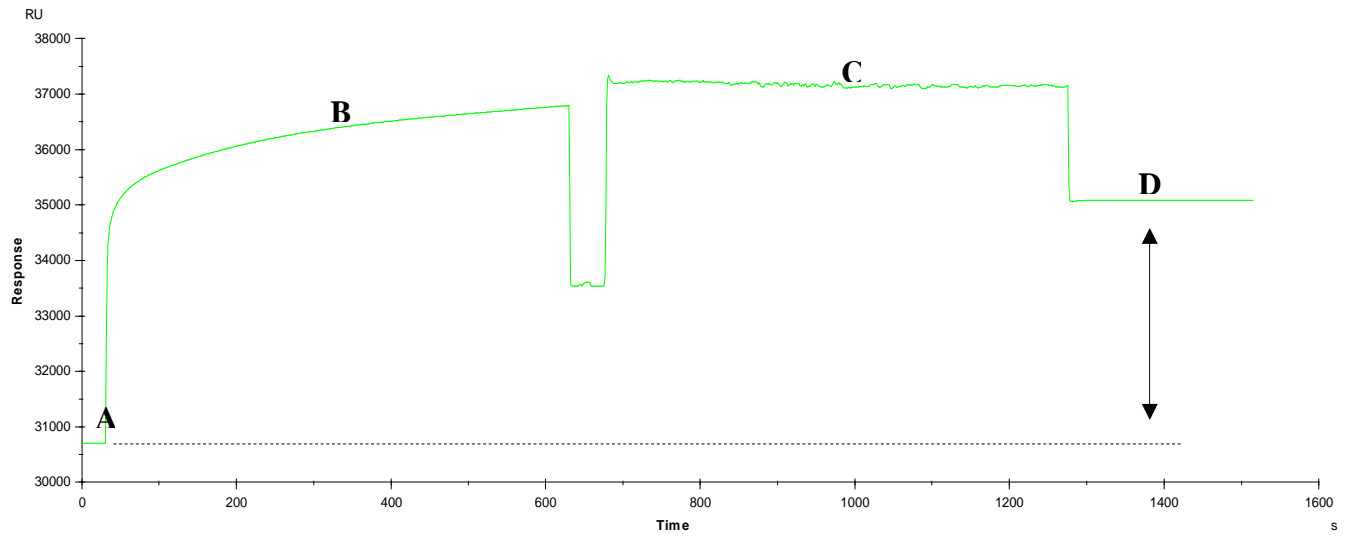


Figure 4.5.2-1: Amine coupling of EGF on L1 sensorchip. **A)** Baseline level. **B)** Activation of the sensor surface with 0.4 M EDC/0.1 M NHS for 7 min. **C)** Binding curve of 100 µg/mL EGF in 10 mM sodium acetate buffer, pH 4.5 injected for 10 min. **D)** Deactivation of the sensor surface with 1 M ethanolamine for 7 min. **E)** Immobilized amount of EGF (**E-A**).

The binding levels of A431 cell lysate in buffer A or B (chapter 3.6.2) followed by 10 min of lipid reconstitution resulted to be much higher on the reference (no EGF immobilised) than on the active surfaces, respectively 4375 RU vs 2180 RU for cell lysate in buffer A and 2462 RU vs 1528 RU for cell lysate in buffer B. As shown in Figure 4.5.2-2, a totally non specific binding of the cell lysate to the sensor chip surface was detected for both utilised cell lysates.

a)



b)

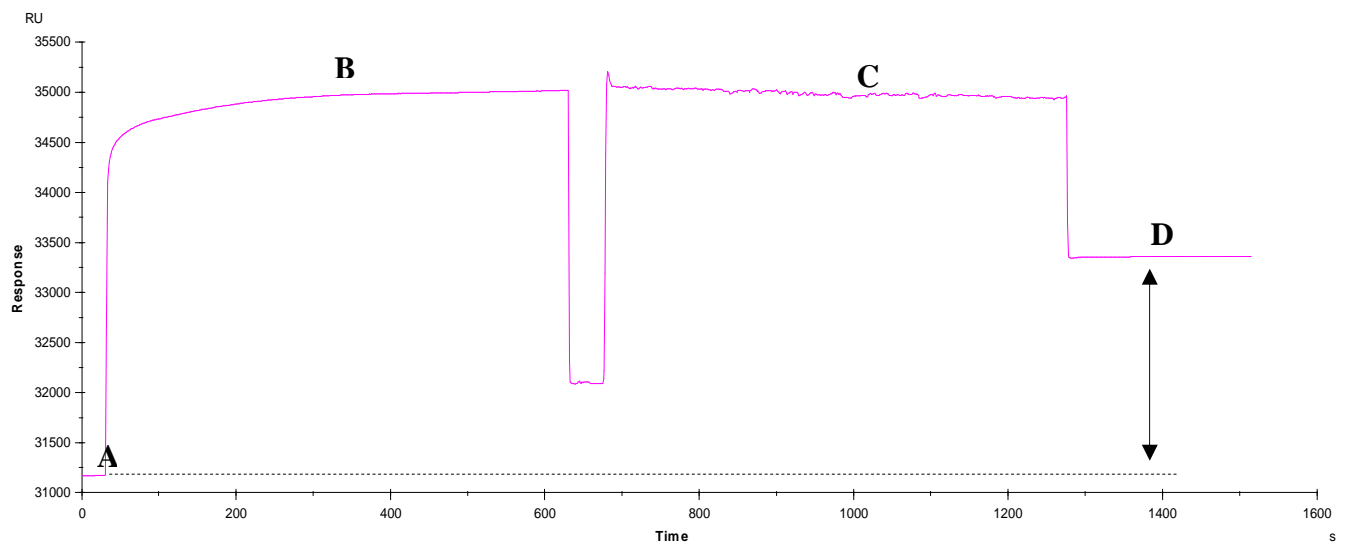


Figure 4.5.2-2: Representative sensograms of reference a) and active b) surfaces showing A431 cell lysate binding to immobilised EGF on L1 sensor chip. **A)** Baseline level. **B)** Cell lysate injection. **C)** Lipid mixture injection. **D)** Binding levels (D-A).

4.5.3 EGF binding to amine coupled purified EGFR

As previously described experiments for EGF/EGFR interaction studies using A431 cell lysate as receptor source didn't give any promising result, we decided to use a commercially available purified form of EGFR purchased from Sigma-Aldrich (St. Louis, MO).

Amine coupling chemistry as described in chapter 3.6.3 was used for the immobilisation on the sensor chip surface and about 3500 RU of EGFR could be immobilized on L1 chip.

The active and reference surfaces were previously conditioned by four consecutive running buffer injections for 7 min at 5 $\mu\text{L}/\text{min}$ and the blank response was obtained.

Increasing concentrations of EGF were subsequently injected at the same conditions over the chip surface. An obvious association to the immobilised EGFR was observed from reference and blank subtracted sensograms (Figure 4.5.3).

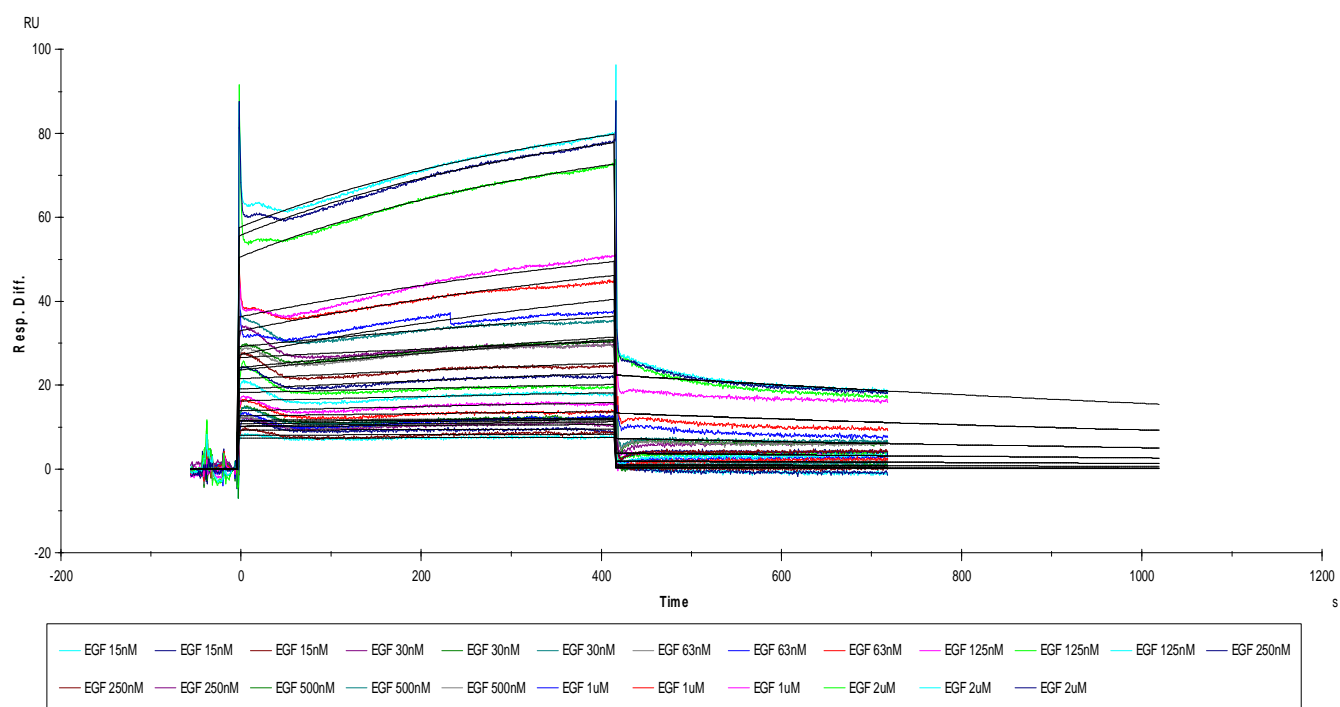


Figure 4.5.3: BIAevaluation curve fit for EGF binding to amine coupled EGFR. Five consecutive blank cycles were run followed by triplicate injections of EGF for 7 min at 5 $\mu\text{L}/\text{min}$ in order of increasing concentration. EGF was allowed to dissociate for 5 min before the surface was regenerated for 1 min with 10 mM glycine, pH 2.0.

EGF binding was concentration dependent and EGF dissociation was observed after 5 min. Kinetic parameters regarding association ($k_a = 1.18 \pm 0.28 \times 10^3 \text{ M}^{-1}\text{sec}^{-1}$) as well as dissociation ($k_d = 4.24 \pm 0.31 \times 10^{-4} \text{ sec}^{-1}$) rate constants were calculated using BIAevaluation 4.1 software and the calculated K_D ($368 \pm 0.65 \text{ nM}$) values, assuming an 1:1 Langmuir binding model, were comparable to those reported in literature for EGF binding to the extracellular ligand binding domain of EGFR [154]. The binding curves behaviour revealed that the association of EGF to the receptor probably triggers higher order events, such as conformational changes, which could interfere with the complex formation.

4. DISCUSSION

The use of agents that target EGFR in cancer therapy has been proposed, and these novel treatment options have been components of an ongoing revolution in cancer therapy, holding the promise of fulfilling significant unmet needs in many tumor types. Of the various EGFR-targeted agents, the most promising and well studied are the mAbs and the small-molecule EGFR tyrosine kinase inhibitors. These agents have shown substantial differences in dosing requirements and toxicity profiles. Nevertheless, both of them have demonstrated little utility as therapeutic agents: monoclonal antibodies are effective at toxic doses, while tyrosine kinase inhibitors result inefficient in colon tumors. The results presented in this thesis work describe the identification of a novel naphthoquinone molecule, FR18, which targets EGFR and induces cell death of HT-29 cells.

As shown in [Figure 4.1](#), the cells are sensitive to FR18 with an approximate IC_{50} ranging from 45.16 to 58.80 μ M. The results obtained in confocal laser scanning microscopy analysis suggest that FR18 binds competitively to the extracellular domain of the receptor. EGF and EGFR form a complex localized in granules in the plasma membrane in EGF-stimulated serum-starved cells, whose presence greatly diminishes in FR18-treated and EGF-stimulated HT-29; the EGF-associated fluorescence signal, in fact, decreases threefold in the presence of FR18, as shown in [Figures 4.2.1 and 4.2.2](#).

This interaction does not prevent the receptor tyrosine kinase activation, assessed in terms of tyrosine phosphorylation ([Figure 4.4](#)), and causes apoptotic EGFR-mediated intracellular signaling ([Figure 4.3](#)).

Apoptotic peaks are detected for higher FR18 concentrations (30 nM-5 μ M) with a peak average of 8.06% for 30 nM FR18 treatment which increases to 26.06% for 5 μ M ([Figure 4.3](#)). Furthermore, the flow cytometric analysis shows that FR18 treatment induces an arrest in the S phase of the cell cycle and that this event together with the observed apoptotic death, is not dose dependent ([Figure 4.3](#)). These results show that FR18, a synthetic small molecule that interferes with EGF binding to EGFR, is able to induce apoptosis in HT-29 cells, suggesting a potential therapeutic application of this compound.

The second aspect of this thesis work concerned the study of EGF/EGFR complex interaction, an important system highly perturbed in several tumor types, by the use of surface plasmon resonance biosensors in order to acquire significant general knowledge that can help the design of new drugs intended to interfere with the EGFR binding activity.

Previously, EGF/EGFR complex interaction was investigated using the total cell lysate of A431 as receptor source. In fact, EGFR immobilisation on the sensor chip surface via two capturing antibodies that recognise its C-terminal region and a lipid bilayer environment reconstitution were

investigated. Also EGF was immobilised in order to evaluate its interaction with the EGFR present in A431 cell lysate.

Both these experimental approaches didn't give any positive results. We weren't able to capture the EGFR on the sensor chip surface probably because of the high composition complexity of A431 cell lysates or because of the improper SPR experimental conditions which negatively affected the procedure. Even when EGF was immobilised on the sensor chip surface for EGFR capturing from A431 cell lysates the results were unsatisfactory, thus indicating that a proper EGFR purification step is necessary for this kind of experimental design.

Subsequently a commercially available purified EGF receptor (Sigma-Aldrich, St. Louis, MO) was immobilised on the sensor chip resulting in about 3500 RU of response. The increasing concentrations of EGF injected over the immobilised receptor revealed that the EGFR was able to bind to EGF with a calculated K_D value of 368 ± 0.65 nM, assuming a 1:1 Langmuir binding model, which is in line with those reported in the literature. The obtained results indicate that the association of EGF to the receptor probably triggers higher order events, such as conformational changes, which could probably interfere with the complex formation, therefore binding specificity as well as improvement of the amount of immobilised EGFR able to interact with EGF represent important steps for better understanding this challenging but crucial receptor-ligand complex interaction.

6. BIBLIOGRAPHY

1. Jemal A, Siegel R, Ward E, Hao Y, Xu J, Thun M. (2009) Cancer statistics, 2009. *CA Cancer J Clin* **59**: 225-49.
2. Levine JS and Ahnen DJ. (2006) Adenomatous polyps of the colon. *NEngl J Med* **355**: 2551-7.
3. Worthley DL, Whitehall VL, Spring KJ, Leggett BA. (2007) Colorectal carcinogenesis: Road maps to cancer. *World J Gastroenterol* **13**: 3784-91.
4. Melissa M, Ahmedin J, Robert AS, Elizabeth W. (2009) Worldwide Variations in Colorectal Cancer. *CA Cancer J Clin* **59**: 366-78.
5. Winawer SJ and Sherlock P. (2007) Colorectal cancer screening. *Best Practice & Res Clin Gastroenterol* **21**:1031-48.
6. Peltomaki P. (2003) Role of DNA mismatch repair defects in the pathogenesis of human cancer. *J Clin Oncol* **21**: 1174-9.
7. Kinzler KW and Vogelstein B. (2002) Colorectal tumors. In Vogelstein B and Kinzler KW eds., *The Genetic Basis of Human Cancer* (2nd ed.) McGraw-Hill, New York.
8. McLellan EA and Bird RP. (1988) Specificity Study to Evaluate Induction of Aberrant Crypts in murine Colons. *Cancer Res* **48**: 6183-6.
9. Cheng L and Lai MD. (2003) Aberrant crypt foci as microscopic precursors of colorectal cancer. *World J Gastroenterol* **9**: 2642-9.
10. Hurlstone DP and Cross SS. (2005) Role of aberrant crypt foci detected using high-magnification-chromoscopic colonoscopy in human colorectal carcinogenesis. *J Gastroenterol Hepatol* **20**: 173-81.
11. Takata M, Yao T, Nishiyama KI, Nawata H, Tsuneyoshi M. (2003) Phenotypic alteration in malignant transformation of colonic villous tumours: with special reference to a comparison with tubular tumours. *Histopathology* **43**: 332-9.
12. Kumar V and Robbins SL. (2007) *Robbins basic pathology*. (8th ed.) Saunders/Elsevier, Philadelphia.
13. Cappell MS. (2005) From colonic polyps to colon cancer: pathophysiology, clinical presentation, and diagnosis. *Clin Lab Med* **25**: 135-77.
14. Galiatsatos P and Foulkes WD. (2006) Familial Adenomatous Polyposis. *The American Journal of Gastroenterology* **101**: 385-98.
15. Kinzler KW and Vogelstein B. (1996) Lessons from hereditary colorectal cancer. *Cell* **87**: 159-70.

16. Powell SM, Zilz N, Beazer-Barclay Y, Bryan TM, Hamilton SR, Thibodeau SN, Vogelstein B, Kinzler KW. (1992) APC mutations occur early during colorectal tumorigenesis. *Nature* **359**: 235-7.
17. Jen J, Powell SM, Papadopoulos N, Smith KJ, Hamilton SR, Vogelstein B, Kinzler KW. (1994) Molecular determinants of dysplasia in colorectal lesions. *Cancer Res* **54**: 5523-6.
18. Smith AJ, Stern HS, Penner M, Hay K, Mitri A, Bapat BV, Gallinger S. (1994) Somatic APC and K-ras codon 12 mutations in aberrant crypt foci from human colons. *Cancer Res* **54**: 5527-30.
19. Korinek V, Barker N, Morin PJ, van Wichen D, de Weger R, Kinzler KW, Vogelstein B, Clevers H. (1997) Constitutive transcriptional activation by a beta-catenin-Tcf complex in APC^{-/-} colon carcinoma. *Science* **275**: 1784-7.
20. Morin PJ, Sparks AB, Korinek V, Barker N, Clevers H, Vogelstein B, Kinzler KW. (1997) Activation of beta-catenin-Tcf signaling in colon cancer by mutations in beta-catenin or APC. *Science* **275**: 1787-90.
21. Smits R, Kielman MF, Breukel C, Zurcher C, Neufeld K, Jagmohan-Changur S, et al. (1999) Apc1638T: a mouse model delineating critical domains of the adenomatous polyposis coli protein involved in tumorigenesis and development. *Genes Dev* **13**: 1309-21.
22. Sparks AB, Morin PJ, Vogelstein B, Kinzler KW. (1998) Mutational analysis of the APC/beta-catenin/Tcf pathway in colorectal cancer. *Cancer Res* **58**:1130-4.
23. Satoh S, Daigo Y, Furukawa Y, Kato T, Miwa N, Nishiwaki T, et al. (2000) AXIN1 mutations in hepatocellular carcinomas, and growth suppression in cancer cells by virus-mediated transfer of AXIN1. *Nat Genet* **24**: 245-50.
24. Clevers H. (2000) Axin and hepatocellular carcinomas. *Nat Genet* **24**: 206-8.
25. Miyoshi Y, Nagase H, Ando H, Horii A, Ichii S, Nakatsuru S, Aoki T, Miki Y, Mori T, Nakamura Y. (1992) Somatic mutations of the APC gene in colorectal tumors: mutation cluster region in the APC gene. *Hum Mol Genet* **1**: 229-33.
26. Knudson AG Jr. (1971) Mutation and cancer: statistical study of retinoblastoma. *Proc Natl Acad Sci U S A* **68**: 820-3.
27. Lamlum H, Ilyas M, Rowan A, Clark S, Johnson V, Bell J, Frayling I, et al. (1999) The type of somatic mutation at APC in familial adenomatous polyposis is determined by the site of the germline mutation: a new facet to Knudson's 'two-hit' hypothesis. *Nat Med* **5**: 1071-5.
28. Albuquerque C, Breukel C, van der Luijt R, Fidalgo P, Lage P, Slors FJ, et al. (2002) The 'just-right' signaling model: APC somatic mutations are selected based on a specific level of activation of the beta-catenin signaling cascade. *Hum Mol Genet* **11**:1549-60.
29. Forrester K, Almoguera C, Han K, Grizzle WE, Perucho M. (1987) Detection of high incidence of K-ras oncogenes during human colon tumorigenesis. *Nature* **327**: 298-303.

30. Vogelstein B, Fearon ER, Hamilton SR, Kern SE, Preisinger AC, Leppert M, Nakamura Y, White R, Smits AM, Bos JL (1988) Genetic alterations during colorectal-tumor development. *N Engl J Med* **319**: 525-32.
31. Beach R, Chan AO, Wu TT, White JA, Morris JS, Lunagomez S, Broaddus RR, Issa JP, Hamilton SR, Rashid A (2005) BRAF mutations in aberrant crypt foci and hyperplastic polyposis. *Am J Pathol* **166**: 1069-75.
32. Kim EC and Lance P. (1997) Colorectal polyps and their relationship to cancer. *Gastroenterol Clin North Am* **26**: 1-17.
33. Vogelstein B, Fearon ER, Kern SE, Hamilton SR, Preisinger AC, Nakamura Y, White R (1989) Allelotyping of colorectal carcinomas. *Science* **244**: 207-11.
34. Jen J, Kim H, Piantadosi S, Liu ZF, Levitt RC, Sistonen P, Kinzler KW, Vogelstein B, Hamilton SR (1994) Allelic loss of chromosome 18q and prognosis in colorectal cancer. *N Engl J Med* **331**: 213-21.
35. Keino-Masu K, Masu M, Hinck L, Leonardo ED, Chan SS, Culotti JG, Tessier-Lavigne M. (1996) Deleted in Colorectal Cancer (DCC) encodes a netrin receptor. *Cell* **87**: 175-85.
36. Cho KR, Oliner JD, Simons JW, Hedrick L, Fearon ER, Preisinger AC, Hedge P, Silverman GA, Vogelstein B. (1994) The DCC gene: structural analysis and mutations in colorectal carcinomas. *Genomics* **19**: 525-31.
37. Heldin CH, Miyazono K, ten Dijke P. (1997) TGF-beta signaling from cell membrane to nucleus through SMAD proteins. *Nature* **390**: 465-71.
38. Duff EK and Clarke AR. (1998) Smad4 (DPC4)--a potent tumour suppressor? *Br J Cancer* **78**: 1615-9.
39. Baker SJ, Fearon ER, Nigro JM, Hamilton SR, et al. (1989) Chromosome 17 deletions and p53 gene mutations in colorectal carcinomas. *Science* **244**: 217-21.
40. Baker SJ, Preisinger AC, Jessup JM, Paraskeva C, Markowitz S, et al. (1990) p53 gene mutations occur in combination with 17p allelic deletions as late events in colorectal tumorigenesis. *Cancer Res* **50**: 7717-22.
41. Lane DP. (1992) Cancer. p53, guardian of the genome. *Nature* **358**: 15-6.
42. Waldman T, Kinzler KW, Vogelstein B. (1995) p21 is necessary for the p53-mediated G1 arrest in human cancer cells. *Cancer Res* **55**: 5187-90.
43. Burns TF and El-Deiry WS. (1999) The p53 pathway and apoptosis. *J Cell Physiol* **181**: 231-9.
44. Ohue M, Tomita N, Monden T, Fujita M, Fukunaga M, Takami K, Yana I, Ohnishi T, et al. (1994) A frequent alteration of p53 gene in carcinoma in adenoma of colon. *Cancer Res* **54**: 4798-804.

45. Yamaguchi A, Makimoto K, Goi T, Takeuchi K, Maehara M, Isobe Y, Nakagawara G. (1994) Overexpression of p53 protein and proliferative activity in colorectal adenoma. *Oncology* **51**: 224-7.
46. Kaklamanis L, Gatter KC, Mortensen N, Baigrie RJ, Heryet A, Lane DP, Harris AL. (1993) p53 expression in colorectal adenomas. *Am J Pathol* **142**: 87-93.
47. Kaserer K, Schmaus J, Bethge U, Migschitz B, Fasching S, Walch A, Herbst F, et al. (2000) Staining patterns of p53 immunohistochemistry and their biological significance in colorectal cancer. *J Pathol* **190**: 450-6.
48. Boland CR, Sato J, Appelman HD, Bresalier RS, Feinberg AP. (1995) Microallelotyping defines the sequence and tempo of allelic losses at tumour suppressor gene loci during colorectal cancer progression. *Nat Med* **1**: 902-9.
49. Lengauer C, Kinzler KW, Vogelstein B. (1998) Genetic instabilities in human cancers. *Nature* **396**: 643-9.
50. Ionov Y, Peinado MA, Malkhosyan S, Shibata D, Perucho M. (1993) Ubiquitous somatic mutations in simple repeated sequences reveal a new mechanism for colonic carcinogenesis. *Nature* **363**: 558-61.
51. Thibodeau SN, Bren G, Schaid D. (1993) Microsatellite instability in cancer of the proximal colon. *Science* **260**: 816-9.
52. Lengauer C, Kinzler KW, Vogelstein B. (1997) Genetic instability in colorectal cancers. *Nature* **386**: 623-7.
53. Burri N, Shaw P, Bouzourene H, Sordat I, Sordat B, Gillet M, Schorderet D, Bosman FT, Chaubert P. (2001) Methylation silencing and mutations of the p14ARF and p16INK4A genes in colon cancer. *Lab Invest* **81**:217-29.
54. Shannon BA and Iacopetta BJ. (2001) Methylation of the hMLH1, p16, and MDR1 genes in colorectal carcinoma: associations with clinicopathological features. *Cancer Lett* **167**: 91-7.
55. Zhu P, Martin E, Mengwasser J, Schlag P, Janssen KP, Göttlicher M. (2004) Induction of HDAC2 expression upon loss of APC in colorectal tumorigenesis. *Cancer Cell* **5**: 455-63.
56. Wilson AJ, Byun DS, Popova N, Murray LB, L'Italien K, et al. (2006) Histone deacetylase 3 (HDAC3) and other class I HDACs regulate colon cell maturation and p21 expression and are deregulated in human colon cancer. *J Biol Chem* **281**:13548-58.
57. Dukes CE. (1932) The classification of cancer of the rectum. *Journal of Pathol Bacteriol* **35**: 323
58. Fauci AS, Braunwald E, Kasper DL, Hauser SL, Longo DL, Jameson JL, and Loscalzo J. (2008) Harrison's Principles of Internal Medicine. (17ed.) McGraw-Hill, USA.
59. Smith AJ, Driman DK, Spithoff K, Hunter A, McLeod RS, Simunovic M, Langer B. (2010) Guideline for optimization of colorectal cancer surgery and pathology. *J Surg Oncol* **101**: 5-12.

60. Wolpin BM, Meyerhardt JA, Mamon HJ, Mayer RJ (2007) Adjuvant Treatment of Colorectal Cancer. *CA Cancer J Clin* **57**: 168-85
61. Asmis TR and Saltz S. (2008) Systemic Therapy for Colon Cancer. *Gastroenterol Clin N Am* **7**: 287-95.
62. Scheithauer W, Rosen H, Kornek GV, Sebesta C, Depisch D. (1993) Randomised comparison of combination chemotherapy plus supportive care with supportive care alone in patients with metastatic colorectal cancer. *BMJ* **306**: 752-5.
63. Nordic Gastrointestinal Tumor Adjuvant Therapy Group. (1992) Expectancy or primary chemotherapy in patients with advanced asymptomatic colorectal cancer: a randomized trial. *J Clin Oncol* **10**: 904-11.
64. Ragnhammer P, Hafström L, Nygren P, Glimelius B for the SBU group. (2001) A systematic overview of chemotherapy effects in colorectal cancer. *Acta Oncol* **40**: 282-308.
65. Krueger GM, Alexander LL, Whippen DA, Balch CM. (2006) Arnoldus Goudsmit, MD, PhD: chemotherapist, visionary, founder of the American Society of Clinical Oncology, 1909-2005. *J Clin Oncol* **24**: 4033-6.
66. Tournigand C, Andre T, Achille E, Lledo G, Flesh M, Mery-Mignard D, Quinaux E, et al. (2004) FOLFIRI followed by FOLFOX6 or the reverse sequence in advanced colorectal cancer: a randomized GERCOR study. *J Clin Oncol* **22**: 229-37.
67. Colucci G, Gebbia V, Paoletti G, et al. (2005) Phase III randomized trial of FOLFIRI versus FOLFOX4 in the treatment of advanced colorectal cancer: a multicenter study of the Gruppo Oncologico Dell'Italia Meridionale. *J Clin Oncol* **23**: 4866-75.
68. Hurwitz H, Fehrenbacher L, Novotny W, et al. (2004) Bevacizumab plus irinotecan, fluorouracil, and leucovorin for metastatic colorectal cancer. *N Engl J Med* **350**: 2335-42.
69. Saltz LB, Meropol NJ, Loehrer PJ Sr, et al. (2004) Phase II trial of cetuximab in patients with refractory colorectal cancer that expresses the epidermal growth factor receptor. *J Clin Oncol* **22**: 1201-8.
70. Cunningham D, Humblet Y, Siena S, et al. (2004) Cetuximab monotherapy and cetuximab plus irinotecan in irinotecan-refractory metastatic colorectal cancer. *N Engl J Med* **351**: 337-45.
71. Van Cutsem E, Peeters M, Siena S, et al. (2007) Open-label phase III trial of panitumumab plus best supportive care compared with best supportive care alone in patients with chemotherapy refractory metastatic colorectal cancer. *J Clin Oncol* **25**: 1658-64.
72. Olayioye MA, Neve RM, Lane HA, Hynes NE. (2000) The ErbB signaling network: receptor heterodimerization in development and cancer. *EMBO Journal* **19**:3159-67.
73. Tzahar E, Waterman H, Chen X, Levkowitz G, Karunagaran D, et al. (1996) A hierarchical network of interreceptor interactions determines signal transduction by Neu differentiation factor/neuregulin and epidermal growth factor. *Mol Cell Biol* **16**:5276-87.

74. Meyerhardt JA, Kwok A, Ratain MJ, McGovren JP, Fuchs CS. (2004) Relationship of baseline serum bilirubin to efficacy and toxicity of single-agent irinotecan in patients with metastatic colorectal cancer. *J Clin Oncol* **22**:1439–46.
75. Cummings RD, Soderquist AM, Carpenter G. (1985) The oligosaccharide moieties of the epidermal growth factor receptor in A-431 cells. Presence of complex-type N-linked chains that contain terminal N-acetylgalactosamine residues. *J Biol Chem* **260**: 11944-52.
76. Ward CW and Garrett TP. (2001) The relationship between the L1 and L2 domains of the insulin and epidermal growth factor receptors and leucine-rich repeat modules. *BMC Bioinformatics* **2**: 4.
77. Lax I, Fischer R, Ng C, Segre J, Ullrich A, Givol D, Schlessinger J. (1991) Noncontiguous regions in the extracellular domain of EGF receptor define ligand-binding specificity. *Cell Regul* **2**: 337-45.
78. Ward CW, Hoyne PA, Flegg RH. (1995) Insulin and epidermal growth factor receptors contain the cysteine repeat motif found in the tumor necrosis factor receptor. *Proteins* **22**: 141-53.
79. Ferguson KM, Berger MB, Mendrola JM, Cho HS, Leahy DJ, et al. (2003) EGF activates its receptor by removing interactions that autoinhibit ectodomain dimerization. *Mol Cell* **11**: 507-17.
80. Ogiso H, Ishitani R, Nureki O, Fukai S, Yamanaka M, et al. (2002) Crystal structure of the complex of human epidermal growth factor and receptor extracellular domains. *Cell* **110**: 775-87.
81. Garrett TP, McKern NM, Lou M, Elleman TC, Adams TE, et al. (2002) Crystal structure of a truncated epidermal growth factor receptor extracellular domain bound to transforming growth factor alpha. *Cell* **110**: 763-73.
82. Stroud RM and Wells JA. (2004) Mechanistic diversity of cytokine receptor signaling across cell membranes. *Sci STKE* 2004, re7.
83. Dawson JP, Berger MB, Lin CC, Schlessinger J, Lemmon MA, et al. (2005) Epidermal growth factor receptor dimerization and activation require ligand-induced conformational changes in the dimer interface. *Mol Cell Biol* **25**: 7734-42.
84. Berezov A, Chen J, Liu Q, Zhang HT, Greene MI, et al. (2002) Disabling receptor ensembles with rationally designed interface peptidomimetics. *J Biol Chem* **277**: 28330-9.
85. Saxon ML and Lee DC. (1999) Mutagenesis reveals a role for epidermal growth factor receptor extracellular subdomain IV in ligand binding. *J Biol Chem* **274**: 28356-62.
86. Dawson JP, Bu Z, Lemmon MA. (2007) Ligand-Induced Structural Transitions in ErbB Receptor Extracellular Domains. *Structure* **15**: 942-54.
87. Burgess AW, Cho HS, Eigenbrot C, Ferguson KM, Garrett TP, et al. (2003) An open-and-shut case? Recent insights into the activation of EGF/ErbB receptors. *Mol Cell* **12**: 541-52.

88. Mattoon D, Klein P, Lemmon MA, Lax I, Schlessinger J. (2004) The tethered configuration of the EGF receptor extracellular domain exerts only a limited control of receptor function. *Proc Natl Acad Sci U S A* **101**: 923-8.
89. Walker F, Orchard SG, Jorissen RN, Hall NE, Zhang HH, et al. (2004) CR1/CR2 interactions modulate the functions of the cell surface epidermal growth factor receptor. *J Biol Chem* **279**: 22387-98.
90. Johns TG, Mellman I, Cartwright GA, Ritter G, Old LJ, et al. (2005) The antitumor monoclonal antibody 806 recognizes a high-mannose form of the EGF receptor that reaches the cell surface when cells overexpress the receptor. *Faseb J* **19**: 780-2.
91. Whitson KB, Whitson SR, Red-Brewer ML, McCoy AJ, Vitali AA, et al. (2005) Functional effects of glycosylation at Asn-579 of the epidermal growth factor receptor. *Biochemistry* **44**: 14920-31.
92. Zhang X, Gureasko J, Shen K, Cole PA, Kuriyan J. (2006) An allosteric mechanism for activation of the kinase domain of epidermal growth factor receptor. *Cell* **125**: 1137-49.
93. Gotoh N, Tojo A, Hino M, Yazaki Y, Shibuya M. (1992) A highly conserved tyrosine residue at codon 845 within the kinase domain is not required for the transforming activity of human epidermal growth factor receptor. *Biochem Biophys Res Commun* **186**: 768-74.
94. Erba EB, Matthiesen R, Bunkenborg J, Schulze WX, Di Stefano P, et al. (2007) Quantitation of multisite EGF receptor phosphorylation using mass spectrometry and a novel normalization approach. *J Proteome Res* **6**: 2768-85.
95. Sebastian S, Settleman J, Reshkin SJ, Azzariti A, Bellizzi A, et al. (2006) The complexity of targeting EGFR signaling in cancer: from expression to turnover. *Biochim Biophys Acta* **1766**: 120-39.
96. Schulze WX, Deng L, Mann M. (2005) Phosphotyrosine interactome of the ErbB-receptor kinase family. *Mol Syst Biol* **1**: 2005.0008.
97. Hynes NE and Lane HA (2005) ERBB receptors and cancer: the complexity of targeted inhibitors. *Nat Rev Cancer* **5**: 341-54.
98. Katso R, Okkenhaug K, Doval DC et al. (2001) Cellular function of phosphoinositide 3-kinases: implications for development, homeostasis, and cancer. *Cell Dev Biol* **17**: 615-75.
99. Downward J. PI3-kinase, Akt, and cell survival. (2004) *Semin Cell Dev Biol* **15**:177-82.
100. Yu H and Jove R. The STATs of cancer - new molecular targets come of age. (2004) *Nature Rev Cancer* **4**: 97-105.
101. Bowman T, Garcia R, Turkson J, Jove R. (2000) STATs in oncogenesis. *Oncogene* **19**: 2474-88.
102. Buettner R, Mora LB, Jove R. (2002) Activated STAT signaling in human tumors provides novel molecular targets for therapeutic intervention. *Clin Cancer Res* **8**: 945-54.

103. Bromberg J and Darnell JE Jr. (2000) The role of STATs in transcriptional control and their impact on cellular function. *Oncogene* **19**: 2468-73.
104. Levy DE and Darnell JE Jr. (2002) Stats: transcriptional control and biological impact. *Nature Rev Mol Cell Biol* **3**: 651-62.
105. Yarden Y and Sliwkowski MX. (2001) Untangling the ErbB signaling network. *Nat Rev Mol Cell Biol* **2**: 127-37.
106. Carpenter G. (2003) Nuclear localization and possible functions of receptor tyrosine kinases. *Curr Opin Cell Biol* **15**: 143-8.
107. Wiley HS. (2003) Trafficking of the ErbB receptors and its influence on signaling. *Exp Cell Res* **284**: 78-88.
108. Stoscheck CM, and Carpenter G. (1984) Characterization of the metabolic turnover of epidermal growth factor receptor protein in A-431 cells. *J Cell Physiol* **120**: 296-302.
109. Waterman H, Sabanai I, Geiger B, Yarden Y. (1998) Alternative intracellular routing of ErbB receptors may determine signaling potency. *J Biol Chem* **273**: 13819-27.
110. Herbst JJ, Opresko LK, Walsh BJ, Lauffenburger DA, Wiley HS. (1994) Regulation of postendocytic trafficking of the epidermal growth factor receptor through endosomal retention. *J Biol Chem* **269**: 12865-73.
111. Futter CE, Pearse A, Hewlett LJ, Hopkins CR. (1996) Multivesicular endosomes containing internalized EGF-EGF receptor complexes mature and then fuse directly with lysosomes. *J Cell Biol* **132**: 1011-23.
112. Chen WS, Lazar CS, Poenie M, Tsien RY, Gill GN, et al. (1987) Requirement for intrinsic protein tyrosine kinase in the immediate and late actions of the EGF receptor. *Nature* **328**: 820-3.
113. Schmidt MH, Furnari FB, Cavenee WK, Bogler O. (2003) Epidermal growth factor receptor signaling intensity determines intracellular protein interactions, ubiquitination, and internalization. *Proc Natl Acad Sci U S A* **100**: 6505-10.
114. Wang Q, Villeneuve G, Wang Z. (2005) Control of epidermal growth factor receptor endocytosis by receptor dimerization, rather than receptor kinase activation. *EMBO Rep* **6**: 942-8.
115. Duan L, Miura Y, Dimri M, Majumder B, Dodge IL, et al. (2003) Cbl-mediated ubiquitinylation is required for lysosomal sorting of epidermal growth factor receptor but is dispensable for endocytosis. *J Biol Chem* **278**: 28950-60.
116. Huang F, Kirkpatrick D, Jiang X, Gygi S, Sorkin A. (2006) Differential regulation of EGF receptor internalization and degradation by multiubiquitination within the kinase domain. *Mol Cell* **21**: 737-48.
117. Levkowitz G, Waterman H, Zamir E, Kam Z, Oved S, et al. (1998) c-Cbl/Sli-1 regulates endocytic sorting and ubiquitination of the epidermal growth factor receptor. *Genes Dev* **12**: 3663-74.

118. Haugh JM, Huang AC, Wiley HS, Wells A, Lauffenburger DA. (1999) Internalized epidermal growth factor receptors participate in the activation of p21(ras) in fibroblasts. *J Biol Chem* **274**: 34350-60.
119. Wang Y, Pennock S, Chen X, Wang Z. (2002) Endosomal signaling of epidermal growth factor receptor stimulates signal transduction pathways leading to cell survival. *Mol Cell Biol* **22**: 7279-90.
120. Hendriks BS, Opresko LK, Wiley HS, Lauffenburger D. (2003) Coregulation of epidermal growth factor receptor/human epidermal growth factor receptor 2 (HER2) levels and locations: quantitative analysis of HER2 overexpression effects. *Cancer Res* **63**: 1130-1137.
121. Wiley HS, Shvartsman SY, Lauffenburger DA. (2003) Computational modeling of the EGF-receptor system: a paradigm for systems biology. *Trends Cell Biol* **13**: 43-50.
122. Carpenter G. (2000) The EGF receptor: a nexus for trafficking and signaling. *Bioessays* **22**: 697-707.
123. de Larco JE and Todaro GJ. (1978) Epithelioid and fibroblastic rat kidney cell clones: epidermal growth factor (EGF) receptors and the effect of mouse sarcoma virus transformation. *J Cell Physiol* **94**: 335-42.
124. Holbro T, Civenni G, Hynes NE. (2003) The ErbB receptors and their role in cancer progression. *Exp Cell Res* **284**: 99-110.
125. Shibamoto S, Hayakawa M, Takeuchi K, Hori T, Oku N, Miyazawa K, et al. (1994) Tyrosine Phosphorylation of β -Catenin and Plakoglobin Enhanced by Hepatocyte Growth Factor and Epidermal Growth Factor in Human Carcinoma Cells. *Cell Adhes Commun* **1**: 295-305.
126. Daniel JM and Reynolds AB. (1997) Tyrosine phosphorylation and cadherin/catenin function. *Bioessays* **19**: 883-91.
127. Herbst RS and Shin DM. (2002) Monoclonal antibodies to target epidermal growth factor receptor-positive tumors: a new paradigm for cancer therapy. *Cancer* **94**: 1593-611.
128. Franovic A, Gunaratnam L, Smith K, Robert I, Patten D, et al. (2007) Translational up-regulation of the EGFR by tumor hypoxia provides a nonmutational explanation for its overexpression in human cancer. *Proc Natl Acad Sci U S A* **104**: 13092-7.
129. McKaya JA, Murraya LJ, Curranb S, Rossb VG, C Clarka, Murrayb GI, Cassidy J, McLeoda HL (2002) Evaluation of the epidermal growth factor receptor (EGFR) in colorectal tumours and lymph node metastases. *EJC* **38**: 2258-64.
130. Nicholson RI, Gee JM, Harper ME. (2001) EGFR and cancer prognosis. *Eur J Cancer* **37** Suppl 4: S9-15.
131. Sizeland AM, and Burgess AW. (1992) Anti-sense transforming growth factor alpha oligonucleotides inhibit autocrine stimulated proliferation of a colon carcinoma cell line. *Mol Biol Cell* **3**: 1235-43.

132. Citri A and Yarden Y. (2006) EGF-ERBB signaling: towards the systems level. *Nat Rev Mol Cell Biol* **7**: 505-16.
133. Sharma SV, Bell DW, Settleman J, Haber DA. (2007) Epidermal growth factor receptor mutations in lung cancer. *Nat Rev Cancer* **7**: 169-81.
134. Lafky JM, Wilken JA, Baron AT, Maihle NJ. (2008) Clinical implications of the ErbB/epidermal growth factor (EGF) receptor family and its ligands in ovarian cancer. *Bioch Bioph Acta* **1785**: 232-65.
135. Mackenzie MJ, Hirte HW, Glenwood G, Jean M, Goel R, et al. (2005) A phase II trial of ZD1839 (Iressa) 750 mg per day, an oral epidermal growth factor receptor-tyrosine kinase inhibitor, in patients with metastatic colorectal cancer. *Invest New Drugs* **23**: 165-70.
136. Townsley CA, Major P, Siu LL, Dancy J, Chen E, Pond GR, Nicklee T, Ho J, Hedley D, Tsao M, Moore MJ, Oza AM. (2006) Phase II study of erlotinib (OSI-774) in patients with metastatic colorectal cancer. *Br J Cancer* **94**: 1136-43.
137. Bardelli A and Siena S. (2010) Molecular Mechanisms of Resistance to Cetuximab and Panitumumab in Colorectal Cancer. *J Clin Oncol* [Epub ahead of print].
138. Shankaran V, Obel J, Benson AB 3rd. (2010) Predicting Response to EGFR Inhibitors in Metastatic Colorectal Cancer: Current Practice and Future Directions. *Oncologist* [Epub ahead of print].
139. Ponz-Sarvisé M, Rodríguez J, Viudez A, Chopitea A, Calvo A, García-Foncillas J, Gil-Bazo I. (2007) Epidermal growth factor receptor inhibitors in colorectal cancer treatment: What's new? *World J Gastroenterol* **13**: 5877-87.
140. Yoon Y, Kim YO, Lim NY, Jeon WK, Sung HJ. (1999) Shikonin, an ingredient of *Lithospermum erythrorhizon* induced apoptosis in HL60 human premyelocytic leukemia cell line. *Planta Med* **65**: 532-5.
141. Singh F, Gao D, Lebwohl M, Wei H. (2003) Shikonin modulates cell proliferation by inhibiting epidermal growth factor receptor signalling in human epidermoid carcinoma cells. *Cancer Lett* **200**:115-21.
142. Nakaya K and Miyasaka T. (2003) A shikonin derivative, beta-hydroxyisovalerylshikonin, is an ATP-non-competitive inhibitor of protein tyrosine kinases. *Anticancer Drugs* **14**: 683-93.
143. Gumireddy K, Baker SJ, Cosenza SC, John P, et al. (2005) A non-ATP-competitive inhibitor of BCR-ABL overrides imatinib resistance. *Proc Natl Acad Sci USA* **102**: 1992-7.
144. Minsky M. (1961) Microscopy Apparatus. US Pat. 3,013,467.
145. Minsky M. (1988) Memoir on Inventing the Confocal Scanning Microscopy. *Scanning* **10**: 128-38.
146. Liedberg B, Nylander C, Lundstrom I. (1983) Surface plasmon resonance for gas detection and biosensing. *Sensors Actuators* **4**: 299-304.

147. Karlsson R. (1999) Affinity analysis of non-steadystate data obtained under mass transport limited conditions using Biacore technology. *J Mol Recognit* **12**:285-92.
148. Mickuviene I, Kirveliėne V, Juodka B. (2004) Experimental survey of nonclonogenic viability assays for adherent cells in vitro. *Toxicol InVitro* **18**: 639-48.
149. Haigler H, Ash J F, Singer S J, Cohen S. (1978) Visualization by fluorescence of the binding and internalization of epidermal growth factor in human carcinoma cells A-431. *Proc Natl Acad Sci U S A* **75**: 3317–21.
150. Yoshimoto Y and Imoto M. (2002) Induction of EGF-Dependent Apoptosis by Vacuolar-Type H⁺-ATPase Inhibitors in A431 Cells Overexpressing the EGF Receptor. *Experimental Cell Research* **279**: 118–27.
151. Stenlund P, Babcock G, Sodroski J, Myszka D. (2003) Capture and Reconstitution of G-protein Coupled Receptors on a Biosensor Surface. *Analytical Biochemistry* **316**: 243-50.
152. Nice E, Lackmann M, Smyth F, Fabri L, Burgess AW. (1994) Synergies between micropreparative high-performance liquid chromatography and an instrumental optical biosensor. *J Chromatogr A* **660**: 69-85.
153. Varkondi E, Schäfer E, Bökönyı G, Gyökeres T, Orfi L, Petak I, Pap A, Szokoloczi O, Keri G, Schwab R. (2005) Comparison of ELISA-based tyrosine kinase assays for screening EGFR inhibitors. *Journal of Receptors and Signal Transduction Res* **25**: 45-56.
154. Zhou M, Felder S, Rubinstein M, Hurwitz DR, Ullrich A, Lax I, Schlessinger J. (1993) Real-Time measurements of kinetics of EGF binding to soluble EGF receptor monomers and dimers support the dimerization model for receptor activation. *Biochemistry* **32**: 8193-8.

ATTACHMENT I: PhD COURSE 2007-2009, LIST OF CONGRESS PARTICIPATIONS

1. SIB 2008, 53° SIB Symposium, Riccione, 2008
F. Di Giorgio, C. Parolin, N. Calonghi, C. Mangano, C. Cappadone, J. Hysomema, C. Boga
L. Masotti
“(R)-9-HSA has a more remarkable antiproliferative effect compare to (S)-9-HSA”
2. SIB 2008, 53° SIB Symposium, Riccione, 2008
F. Di Giorgio, N. Calonghi, C. Cappadone, J. Hysomema, C. Mangano, C. Parolin, C.
Stefanelli, M. Zini, M Voltattorni, L. Masotti
“Antitumor activity of new substituted 3-(5-imidazo[2,1-b]thiazolylmethylene)-2-
indolinones”
3. SIB 2008, 53° SIB Symposium, Riccione, 2008
C. Parolin, N. Calonghi, C. Cappadone, F. Di Giorgio, J. Hysomema, C. Mangano, V.
Andrisano, J. Fiori, L. Masotti
“Effect of an indole-derivative in human ovarian carcinoma cells”
4. SIB 2008, 53° SIB Symposium, Riccione, 2008
C. Mangano, N. Calonghi, C. Parolin, C. Cappadone, F. Di Giorgio, J. Hysomema, M.L.
Bolognesi, C. Melchiorre, L. Masotti
“Cytotoxicity evaluation of a polyamine-quinone library conjugates in human colon
carcinoma cells”
5. SIB 2008, 53° SIB Symposium, Riccione, 2008
C. Parolin, N. Calonghi, M. Naldi, C. Mangano, F. Di Giorgio, J. Hysomema, C.
Cappadone, V. Andrisano, A. Mai, L. Masotti
“Histone post-translational modifications by HPLC-ESI-MS after HT29 cell treatment with
HDACs inhibitors”
6. SIB 2008, 53° SIB Symposium, Riccione, 2008
C. Mangano, N. Calonghi, M. Naldi, F. Di Giorgio, J. Hysomema, C. Parolin, C.
Cappadone, A. Mai, L. Masotti
“Biological effects of a new class I HDAC selective inhibitor in HT29 colon cancer cells”

7. SIB 2009, 54° SIB Symposium, Catania, 2009

C. Cappadone, N. Calonghi, J. Hysomema, C. Parolin, G. Sartor, L. Masotti

“Effect of an indole-derivative in human ovarian carcinoma cells”

ACKNOWLEDGEMENTS

A very special thanks goes to Professor Lanfranco Masotti, without whose help I couldn't have had the possibility to conclude this academic experience. I am grateful to Dr. Natalia Calonghi for the advice and guidance in the preparation of this thesis work. I particularly thank Dott.ssa Concettina Cappadone for advising and encouraging me in every moment during our work together. Thanks to Dott.ssa Carola Parolin and Dott.ssa Chiara Mangano who splendidly welcomed me as a colleague and became my friends.

I would also like to thank Professor Helena Danielson, Department of Biochemistry and Organic Chemistry, Uppsala University, Uppsala (Sweden), for generously hosting me in her laboratory and Dott. Tony Christopeit for supervising my SPR work on EGF/EGFR complex.